THE UNIVERSITY OF CHICAGO

SK2 CHANNEL AND METABOTROPIC RECEPTOR MEDIATED REGULATION OF INTRINSIC EXCITABILITY IN PURKINJE CELLS AND IMPLICATIONS FOR CEREBELLAR LEARNING

A DISSERTATION SUBMITTED TO
THE FACULTY OF THE DIVISION OF THE BIOLOGICAL SCIENCES
AND THE PRITZKER SCHOOL OF MEDICINE
IN CANDIDACY FOR THE DEGREE OF
DOCTOR OF PHILOSOPHY

COMMITTEE ON NEUROBIOLOGY

BY
GABRIELLE WATKINS

CHICAGO, ILLINOIS
MARCH 2021

TABLE OF CONTENTS

LIST OF FIGURES

LIST OF ABBREVIATIONS

ACSF Artificial Cerebrospinal Fluid

AHP Afterhyperpolarization

AMPA α-amino-3-hydroxy-5-methyl-4-isoxazolepropionic acid

ATP Adenosine Triphosphate

$CaCl_2$ Calcium Chloride

CamKII Ca^{2+}/Calmodulin-Dependent Protein Kinase II

cAMPS Rp-Adenosine 3,5-cyclic monophosphorothioate triethylammonium salt

CF Climbing Fibers

CO_2 Carbon Dioxide

CR Conditioned Response

DHPG Dihydroxyphenylglycine

EPSC Excitatory Post-Synaptic Current

GABA γ-aminobutyric acid

GPCR G-Protein-Coupled Receptor

GTP Guanosine Triphosphate

HEPES 4-(2-hydroxyethyl)-1-piperazineethanesulfonic acid

IP Intrinsic Plasticity

KCl Potassium Chloride

KOH Potassium Hydroxide

L7-SK2 $SK2^{loxP/loxP}$ L7-Cre^{+}

LTD Long-Term Depression

LTP Long-Term Potentiation

M1-M5 mACHR Subtypes 1-5

mAChR Muscarinic Acetylcholine Receptor

mAHP Medium Afterhyperpolarization

$MgCl_2$ Magnesium Chloride

mGluR1 Metabotropic Glutamate Receptor 1

$MgSO_4$ Magnesium Sulfate

Na_2PO_4 Sodium Phosphate

NaCl Sodium Chloride

$NaHCO_3$ Socium Bicarbonate

NMDA N-methyl-D-aspartate

O_2 Oxygen

oxo-m oxotremorine-m

p Postnatal

PC Purkinje Cells

PF Parallel Fibers

PKA Protein Kinase A

SD Somatic Depolarization Tetanization Protocol

SEM Standard Error of the Mean

SK Small-Conductance Calcium Activated Potassium Channel

SK2 SK Channel Subtype 2

Syn Synaptic Tetanization Protocol

WT Wild-Type

ACKNOWLEDGMENTS

First of all, I would like to thank Christian Hansel for his indispensable support, guidance, and patience in helping me learn how to develop and carry out experiments that address the questions we are both interested in answering. I would not have been able to complete this project without the support of all members of the Hansel Lab, past and present – special thanks to Heather Titley for taking time from her own innumerable experiments to train, mentor, and commiserate with me; Giorgio Grasselli for always having an answer to my most mundane technical questions, and sharing the best methods for looking up the answers on my own; Dana Simmons for her truly incomparable attitude and determination; and Daniel Gill for being open to bouncing all sorts of ideas off of, whether strictly research related or of a more general nature. Thank you to Silas Busch, Tuan Pham, and Ting Feng-Lin for continuing to make the lab one of the truly best research environments I've ever had the privilege to work in.

I am also indebted to my thesis committee: Ruth Anne Eatock, Dan McGehee, and Wei Wei for making the time and effort to carefully consider my work as I've presented it to them, and make suggestions that have significantly contributed to both the results and my development as a scientist.

Thank you to my family for supporting my interests and the occasionally indirect means with which I have pursued them. Snobbit and Munchkin – you are the best siblings anyone could hope for. I am grateful every day that I am your big sister and get to watch you continue to grow into yourselves. Mom and Dad, thank you for encouraging me to follow up on the classes that made me come home and rattle on endlessly with excitement.

Last but not least, thank you to my support network of friends scattered physically further than we would sometimes like, but always reliable – even, at times, when I don't know yet know I need you. You have helped rescue me from more chaos than one normally signs up for through sheer force of generosity, open-mindedness, and a never-ending supply of pet photos.

TECHNICAL ABSTRACT

The question of how the brain processes and records experiences for future recall is crucial to understanding learning and behavior. Traditionally, this has been thought to rely on synaptic plasticity – changes in the connections *between* individual neurons – that lead to the emergence of groups of cells that encode a particular salient feature known as the engram. Attention has recently been drawn to the fact that intrinsic plasticity, or experience-driven changes in the membrane excitability of *individual* neurons may also play a critical role in the proper function of learning. In light of this information, it is important to understand the mechanisms that contribute to this phenomenon.

Activity of small-conductance calcium activated potassium (SK) channels, specifically their downregulation, is known to be required for the regulation of certain forms of cellular excitability such as firing rate and the size of the mAHP. In the cortex and hippocampus, activation of muscarinic acetylcholine receptors (mAChRs) has been shown both to inhibit SK channel activity, and facilitate both cellular excitability *in vitro* and acquisition of learned behavior *in vivo*. And yet, the precise mechanism by which SK channels are downregulated in response to activity during learning, and how this process is facilitated by mAChR activity remains unclear.

In order to address this question the following experiments use a combination of whole-cell patch-clamp recordings from Purkinje cells with pharmacological and genetic manipulations, as well as behavioral experiments focusing on cerebellum-dependent associative learning. The cerebellum is an especially attractive system with which to study intrinsic plasticity and its effect on learning because its circuitry is well understood, and a number of clear behaviors that are easy to observe and measure have been shown to rely on this structure.

Purkinje cells – the sole output neuron of the cerebellum, and therefore responsible for generating behavior – express only the SK2 isoform of SK channels. Following tetanization with both a previously characterized somatic depolarization (SD) protocol, as well as a more physiologically relevant synaptic protocol known to induce long-term potentiation (LTP) at the Purkinje cell-parallel fiber synapse, a stable, significant increase in the evoked firing rate, as well as a decrease in the SK2-channel mediated AHP minimum amplitude were observed in Purkinje cells

recorded from the cerebellar vermis. These effects were significantly enhanced when a G_q-coupled metabotropic agonist was applied in conjunction with the synaptic protocol; but there was no effect of metabotropic activity on SD-induced plasticity. Additionally, changes in cellular excitability were absent in recordings made using mice expressing a Purkinje-cell specific SK2 channel knockout. One downstream effect of G_q-signaling pathway is an increase in PKA activity, which is necessary for internalization of SK2 channels. Expression of intrinsic plasticity in Purkinje cells was also blocked in the presence of an intracellular PKA inhibitor. These experiments suggest one mechanism by which experience-dependent activity might lead to changes in the intrinsic excitability of neurons.

To further characterize the role of intrinsic plasticity in encoding learning, *in vitro* whole-cell patch-clamp recordings were made from mice two days after delay-eyeblink conditioning training, a form of associative learning which is dependent on proper function in lobule HVI of the cerebellum. In recordings from animals that successfully acquired the conditioned response, a significant reduction in the SK2 mediated AHP was observed in response to both synaptic stimulus and evoked activity. Additionally, induction of intrinsic plasticity using the SD protocol, as measured by the change in evoked firing rate relative to baseline, was blocked in conditioned animals. These changes in cellular excitability were absent in pseudoconditioned animals, which received a sham training.

Taken together the results of these experiments provide further insights into the the processes that lead to the induction and expression of intrinsic plasticity throughout the cerebellum. They also suggest that activity-driven changes in cellular excitability are not limited to a timescale of minutes or hours, but instead last on the order of days, and may therefore be relevant to help maintain learning.

CHAPTER 1

GENERAL INTRODUCTION AND BACKGROUND

1.1 LEARNING & MEMORY

Learning – or the ability to adapt and respond to an environment and surrounding stimuli; and memory – the ability to appropriately recall learned responses – are crucial for the competition and survival of any organism. One of the long-standing goals of neuroscience research has been to gain a better understanding of the mechanisms that allow neurons to give rise to these processes, especially because dysfunction has been associated with a range of pathologies including addiction, neuro-developmental disorders, and mental illness in both human studies and animal models. Although much interesting work has been done on how larger patterns of activity in specific regions of the brain give rise to different behaviors, the importance of experience-dependent changes at the cellular level to learning and memory should not be overlooked.

Synaptic vs. Cell-Intrinsic Learning

The canonical understanding of cellular learning is based on synaptic plasticity – that increasing the strength of signaling between one neuron and another through long-term potentiation (LTP), or decreasing the strength via long-term depression (LTD), allows for corresponding changes in both the sensitivity and response to a broad range of stimuli. Proper function of both LTP and LTD have also been shown to be necessary for development during postnatal critical periods (Bi and Poo, 1998; Park et al., 2019). The robust body of work into synaptic plasticity has converged on the importance of NMDA and AMPA receptors in its generation and maintenance, though the expression, and the impact on behavior, can be modified via activation of numerous other receptors. Additionally, increased Ca^{2+} influx through NMDA receptors activates an intracellular signaling pathway involving CamKII that leads to changes in gene expression necessary for LTP maintenance.

Although components of synaptic plasticity induction and maintenance have been shown to

rely on intracellular signaling, and much of the data establishing the role of synaptic plasticity in learning and memory has been obtained using single-cell recordings, there has not been a significant focus on how changes in the fundamental properties of a single cell allow for learning and memory acquisition. Early work from Alkon et al. (1982) and Moyer et al. (1996) was among the first to look at how changes in the membrane excitability and firing rates of individual neurons, or intrinsic plasticity, could be induced in parallel with and function in a complementary manner to synaptic plasticity; and a growing body of subsequent research has looked at activity-induced shifts in measurements such as action potential firing threshold, spontaneous and evoked firing rates, and conductances, continuing to build on the initial findings. Still, the precise mechanisms that give rise to these changes and the conditions under which they occur remain mostly ill-defined.

While behavioral experiments have shown that intrinsic plasticity does accompany learning (Schreurs et al., 1998), and that pharmacological manipulations that either inhibit or facilitate cellular excitability have a corresponding effect on learning (Crestani et al., 2019), the pathway that generates this relationship remains largely elusive. In much the same way, *in vitro* experiments that have finer control over isolating putative individual steps of a molecular pathway have mostly been limited in their ability to relate specific manipulations of intrinsic plasticity expression to broader behavioral outcomes (Debanne and Russier, 2019). Therefore, the precise nature of the interplay between synaptic and intrinsic plasticity, and how it affects learning and memory, remains to be established.

Intrinsic Plasticity & The Engram

Although lesion studies have established that specific regions of the brain need to be intact for normal learning to occur, several papers have demonstrated that not every neuron in a particular region is involved in encoding a learned experience. Rather, learning, and the subsequent memory trace, is encoded in a discrete subpopulation of neurons often referred to as an engram. One view of how intrinsic and synaptic plasticity coordinate to allow learning is that increased neuronal excitability increases the likelihood of either LTP or LTD occurring between two cells via spike-timing de-

pendent plasticity, and that the allocation of neurons to the engram is ultimately determined by changes in synaptic weights (Josselyn and Tonegawa, 2020; Yiu et al., 2014)

A separate emerging and promising theory is the "neurocentric model", which posits that, while synaptic plasticity adjusts the weights between individual neurons, the post-synaptic cell can itself adjust its response to all inputs (Titley et al., 2017).

1.2 THE CEREBELLUM

One of the hurdles to better understanding how learning occurs on a cellular level is that while, broadly speaking, neurons throughout the brain share fundamental properties (e.g. negative resting membrane potential, receptor membrane trafficking, use of Ca^{2+} as a second messenger, among others), the various regions of the brain that are associated with specific forms of learning are difficult to access through available experimental means, either because they are physically difficult to perform surgeries on, or precise genetic targeting tools are not readily available. Moreover the accepted behavioral assays that provide a readout of cellular activity may be difficult either to quantify, or to carry out in a way that guarantees recruitment primarily of the target area. The cerebellum, which is one of the most highly conserved structures throughout vertebrate evolution, provides an ideal model system with which to study cellular learning, due to both its highly organized and tractable architecture, and well-established necessity for several forms of learning.

Architecture

The cerebellum is primarily associated with motor circuitry, although it has also been shown to be involved in cognitive function and cortical processing (Gao et al., 2012; Wagner and Luo, 2019). The key components of the cerebellar system are the Purkinje cells – large, inhibitory neurons with highly developed and morphologically diverse dendritic arborization, which provide the sole output of the structure. Purkinje cells (PC) are located in a single layer throughout the foliated lobules of the cerebellum between the granule cell layer and molecular layer, into which Purkinje cell dendrites are projected. Sensory input arrives from several diverse regions, including the

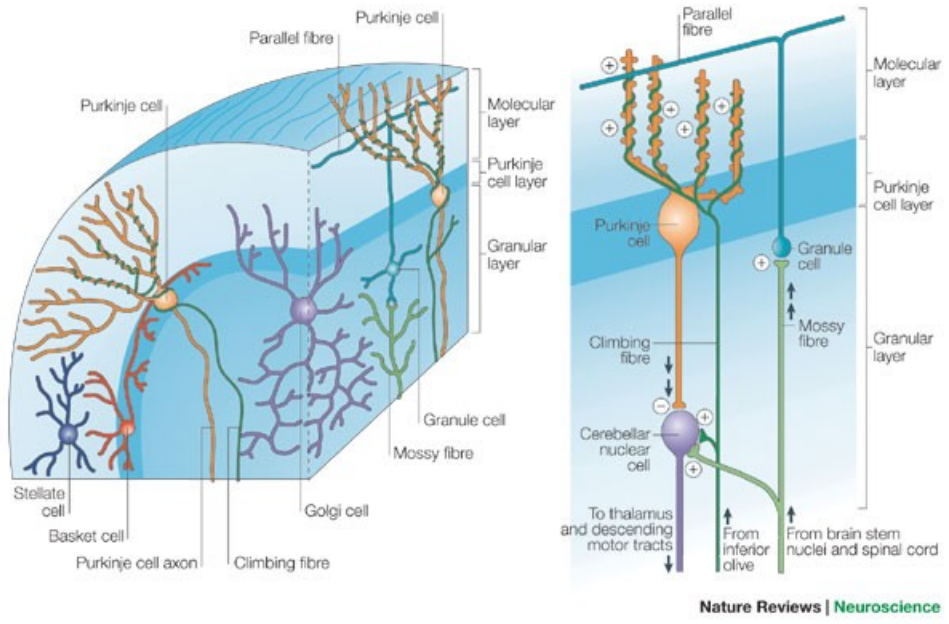

Figure 1.1 – Cerebellar inputs and structure. Adapted from Apps and Garwicz (2005)

motor/premotor and primary/secondary sensory cortices, as well as visual input from the posterior parietal lobe. This information is conveyed from the pons through the mossy fibers, which make synapses with both inhibitory Golgi cells and the small, incredibly numerous granule cells. The axons of the granule cells project upward into the molecular layer as parallel fibers (PF), which form excitatory synapses with Purkinje cells.

The cerebellum also receives input from the inferior olive, a nucleus in the brain stem which forms direct synapses with Purkinje cells through climbing fibers (CF). In comparison to the PF-PC synapse, at which individual cells can receive input from hundreds of PF's, each Purkinje cell receives usually just one climbing fiber input, which makes hundreds of synapses along the proximal dendrite. The CF-PC synapse generates a massive excitatory all-or-none signal resulting in a complex spike – a sodium spike followed by a burst of smaller spikelets – followed by a pause in simple spike firing.

Purkinje cells project into the cerebellar nuclei, and the pause following the CF-induced complex spike acts as a "release" on the firing of target cells.

Cerebellum-dependent Learning

The cerebellum has been implicated in many different forms of motor learning, including the vestibulo-ocular and optokinetic reflexes, which help stabilize the retinal image during movement (Ito, 1998), coordination and balance in tasks such as the Erasmus ladder and rotarod (Brunner and Altman, 1973; Van Der Giessen et al., 2008); and delay eyeblink-conditioning (McCormick and Thompson, 1984). The majority of this research, however, has focused on changes in synaptic plasticity, particularly at the parallel fiber to Purkinje cell (PF-PC) synapse. In the cerebellum, unlike many other areas of the brain, LTD, rather than LTP is associated with successful learning (Jörntell and Hansel, 2006). Coincident activation of the climbing fiber input along with the parallel fibers leads to an influx of Ca^{2+} sufficient to release the Mg^{2+} block from the NMDA receptors, leading to further Ca^{2+} necessary for LTD. Aberrant development resulting in impaired synaptic function has been shown to result in deficits in cerebellum dependent motor learning. Preliminary work looking at intrinsic plasticity and learning in the cerebellum has not yielded consensus on the function of this phenomenon, with researchers reporting both increases (Grasselli et al., 2020; Schreurs, 2019) and decreases (Shim et al., 2017) in intrinsic properties of neurons not limited to Purkinje cells in response to experience-dependent activity.

Clarifying the mechanisms that contribute to the expression of intrinsic plasticity in general, and the role of intrinsic plasticity in cerebellar learning in particular, will help to further elucidate the purpose of this phenomenon, and how it works alongside synaptic plasticity to shape learned behavior.

CHAPTER 2

MECHANISMS OF EXPRESSION & MODULATION OF INTRINSIC PLASTICITY IN CEREBELLAR PURKINJE CELLS

2.1 RATIONALE

In order to gain a more comprehensive insight into how cell-intrinsic changes in excitability function and complement synaptic plasticity, it is important to understand precisely what inputs give rise to these changes and how they can be modulated. Using a combination of genetic and pharmacological manipulations along with whole-cell patch-clamp recording, allows more precise access to the molecular pathways that are necessary for expression of intrinsic plasticity. By performing *in vitro* slice electrophysiology experiments, long-term changes in the firing rate and membrane properties of single Purkinje cells can be measured following stimulation.

2.2 MATERIALS & METHODS

Animals

All procedures were approved by and performed in accordance with the guidelines of the Animal Care and Use Committee of the University of Chicago. Experiments were performed using both male and female mice aged p21-49 of the (C57BL/6J) background obtained from Jackson Laboratory. Purkinje-cell specific knockout mice ("L7-SK2": $SK2^{loxP/loxP}$ L7-Cre^{+}) were generated according to Grasselli et al. (2020). The genotypes of the L7-SK2 strain were analyzed based on tail genomic DNA by a commercial genotyping service (Transnetyx) using primers as defined in Grasselli et al. (2020).

Dissections & Slice Preparation

Animals were anesthetized with isoflurane and immediately decapitated. The cerebellum was removed and the vermis isolated in ACSF cooled to 1-4°C, and containing (in mM): 124 NaCl, 5

KCl, 1.25 Na_2PO_4, $2CaCl_2$, 2 $MgSO_4$, 26 $NaHCO_3$, and 10 D-glucose, bubbled with 95% O_2 and 5% CO_2. Parasagittal slices (200–250 µm) were prepared with a Leica VT-1000S vibratome. All slices were incubated for at least 1 hr at room temperature in oxygenated ACSF.

Electrophysiology

Slices were continuously perfused with ACSF containing picrotoxin (100 µM, Sigma Aldrich) to block $GABA_A$ receptors, and held at near-physiological temperature (32–34 °C) over the course of the experiments. Slices were visualized using a x40 objective mounted on either a Zeiss Examiner A1 microscope or a Zeiss Axioskop2 FS plus microscope (Carl Zeiss MicroImaging). Recordings were made from Purkinje cells located throughout all lobules of the vermis using an EPC-10 amplifier (HEKA Electronics). Currents were filtered at 3kHz, sampled at 20kHz, and acquired using Patchmaster software (HEKA Electronics). The access resistance was compensated (70-80%) in current clamp mode, and hyperpolarizing bias currents were applied to hold the membrane potential around -70 mV. Cells were excluded if the bias current >1nA. Patch pipettes (resistance 2–6 MΩ) were filled with internal solution containing (in mM): 120 K-gluconate, 9 KCl, 10 KOH, 3.48 $MgCl_2$, 10 HEPES, 4 NaCl, 4 Na_2ATP, 0.4 Na_3GTP, and 17.5 sucrose, with the pH adjusted to 7.25-7.35.

In order to ensure that results were due to experimental manipulation and not region-specific variations in excitability, recordings were initially separated into Purkinje cells from Lobules IX-X, where mAChR expression is localized (Rinaldo and Hansel, 2013), or Lobules I-VIII. Data were subsequently pooled where appropriate.

Evoked activity was determined by holding Purkinje cells at -70 mV in current clamp mode and applying a 500 ms depolarization step that gradually increased in 50 pA intervals. Parallel fibers were stimulated by placing a glass pipette filled with ACSF in the molecular layer around the distal dendrites of the Purkinje cell while held at -70mV. The input resistance was monitored throughout the experiments by applying hyperpolarizing current steps (-100 pA) at the end of each sweep. Cells were excluded if the input or holding potential changed by ≥15% over the course of

the baseline.

Intrinsic plasticity was monitored during the test periods by injecting a 500 msec depolarizing current (300-800 pA) to evoke action potentials; during the baseline period, the variation in the number of evoked action potentials could not exceed $\pm 15\%$. During the somatic depolarization (SD) protocol, a 100 msec depolarizing injection between 500pA and 1nA was applied through the recording electrode to the soma at 5 Hz for 8 seconds. For the Synaptic (Syn) protocol, 8 extracellular pulses were used to stimulate parallel fiber bundles at 1Hz for 5 minutes (Fig. 2.1). Parallel fiber EPSC's were confirmed to be $\geq$200pA in voltage clamp mode prior to tetanization. Although the duration of the synaptic protocol is longer than that of the SD protocol, the time series plots in all figures are shown with beginning of the post-induction periods aligned to allow for better visual comparison of IP expression. All drugs were purchased from Sigma or Tocris.

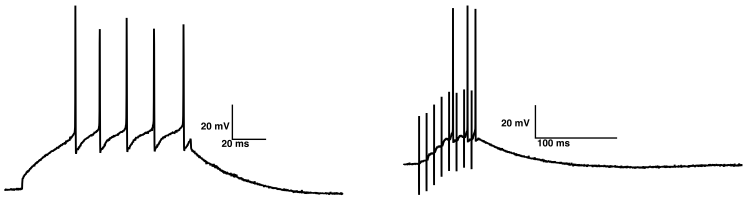

Figure 2.1 – Tetanization protocols. Individual sweeps of the SD (left) and synaptic (right) protocols.

Pharmacology

Drug	Concentration	Function	Application
cAMPS	50 µM	PKA Inhibitor	Intracellular
DAU-5884	1 µM	M3 Antagonist	5 min Wash-on
DHPG	100 µM	mGluR Agonist	5 min Wash-on
oxo-m	7 µM	mAChR Agonist	5 min Wash-on
telenzepine	100 nM	M1 Antagonist	5 min Wash-on

Figure 2.2 – List of drugs used during pharmacological experiments Table shows the drug used and final concentration and application during the experiment; as well as the function of the drug.

Data Analysis

Cellular data were analyzed using RStudio (RStudio, PBC). All data are expressed as mean ± SEM. Statistical analyses were performed using the Mann-Whitney *U* test (between groups), paired Student's *t* test (within subjects), and two-way repeated-measures ANOVA tests as appropriate. Statistical comparisons were based on the number of cells recorded from.

2.3 INTRINSIC PLASTICITY CAN BE INDUCED THROUGH PHYSIOLOGICALLY RELEVANT STIMULI

Previous work characterizing the mechanisms that give rise to intrinsic plasticity in Purkinje cells has relied on induction via a somatic depolarization (SD) protocol (Belmeguenai et al., 2010), which generates a robust and stable increase in the evoked firing rate (Fig. 2.3*B, E*: Lobules IX/X 162.4 ± 10.8% baseline, paired Student's *t* test, p = 2.2×10^{-7}, n = 9; Lobules I-VIII 161.1 ± 11.3% baseline, paired Student's *t* test, p = 2.2×10^{-7}, n = 5). Although this method is reliable, it is also highly artificial, and leaves open the question of how changes in Purkinje cell excitability could be induced under more behaviorally relevant conditions.

One site of synaptic plasticity in the cerebellum is at the parallel fiber-Purkinje cell synapse. A physiologically relevant burst stimulation of presynaptic parallel fiber inputs has been shown to generate LTP at the PF-PC synapse (Lev-Ram et al., 2002). In order to determine whether intrinsic plasticity can also be induced in parallel with synaptic plasticity, recordings were made from Purkinje cells following application of this synaptic (Syn) protocol. The data show that synaptic input leads to a significant increase in the evoked firing rate of Purkinje cells relative to the baseline (Fig. 2.3*B, E*: Lobules IX/X 137.7 ± 9.0% baseline, paired Student's *t* test, p = 2.0×10^{-5}, n = 11; Lobules I-VIII 136.3 ± 12.5% baseline, paired Student's *t* test, p = 3.0×10^{-6}, n = 6). Under control conditions, Purkinje cells do not significantly change their evoked firing rate (96.6 ± 2.1% baseline, paired Student's *t* test p = 0.11, n = 6), and both the SD and synaptic protocols led to a significant increase in firing relative to the control (Fig. 2.3*C, F*: Lobules IX/X ctrl-syn p = 0.008, ctrl-SD p = 0.008, Mann-Whitney U test; Lobules I-VIII ctrl-syn p = 0.008,

ctrl-SD $p = 0.008$, Mann-Whitney U test).

Although both tetanization procedures led to IP expression, across all lobules of the cerebellar vermis, the SD protocol consistently led to a significantly greater increase in the evoked firing rate than synaptic protocol (Fig. 2.3*C, F*: Lobules IX/X syn-SD $p = 0.008$, Mann-Whitney U test; Lobules I-VIII syn-SD $p = 0.008$, Mann-Whitney U test).

In addition to an increase in evoked firing, a significant reduction in the AHP amplitude following depolarization was also observed in the same groups of cells in response to both the synaptic and SD protocols (Fig. 2.4 *B, E*: Lobules IX/X: SD 77.0 $\pm$ 7.2% baseline, $p = 1.8\times10^{-6}$; syn 82.8 $\pm$ 6.8% baseline, $p = 4.6\times10^{-7}$; Lobules I-VIII: SD 77.1 $\pm$ 6.9% baseline, $p = 7.7\times10^{-6}$; syn 93.7 $\pm$ 6.9% baseline, $p = 0.002$, paired Student's t test). As observed with the change in evoked firing, the decrease in AHP was significantly stronger in response to the SD, rather than the synaptic protocol (Fig. 2.4 *C, F*: Lobules IX/X syn-SD p = 0.008; Lobules I-VIII syn-SD p = 0.008, Mann-Whitney U test).

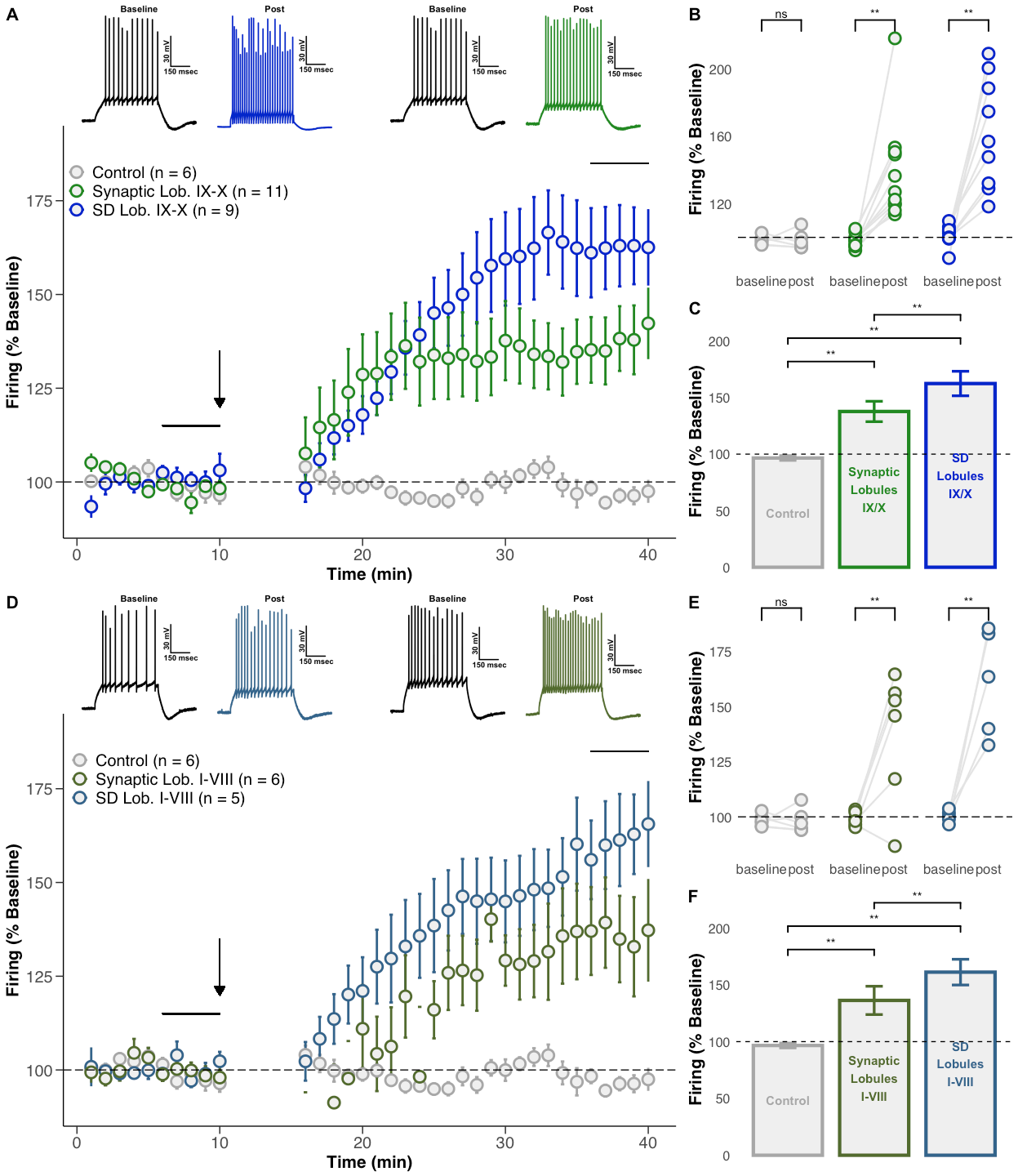

Figure 2.3 – Intrinsic plasticity is evoked in response to synaptic input. ***A, D.*** Time series graph and representative traces showing IP in response to SD and synaptic protocols across the cerebellum. Horizontal lines indicate baseline/post time windows used for statistical analysis. Arrow indicates protocol onset. ***B, E.*** IP expression of individual cells in response to SD or synaptic protocols. ***C, F.*** Average change in evoked firing rate of groups depicted in time series graph. Data are presented as mean ± SEM. *Significance of $p<0.05$, **Significance of $p<0.01$.

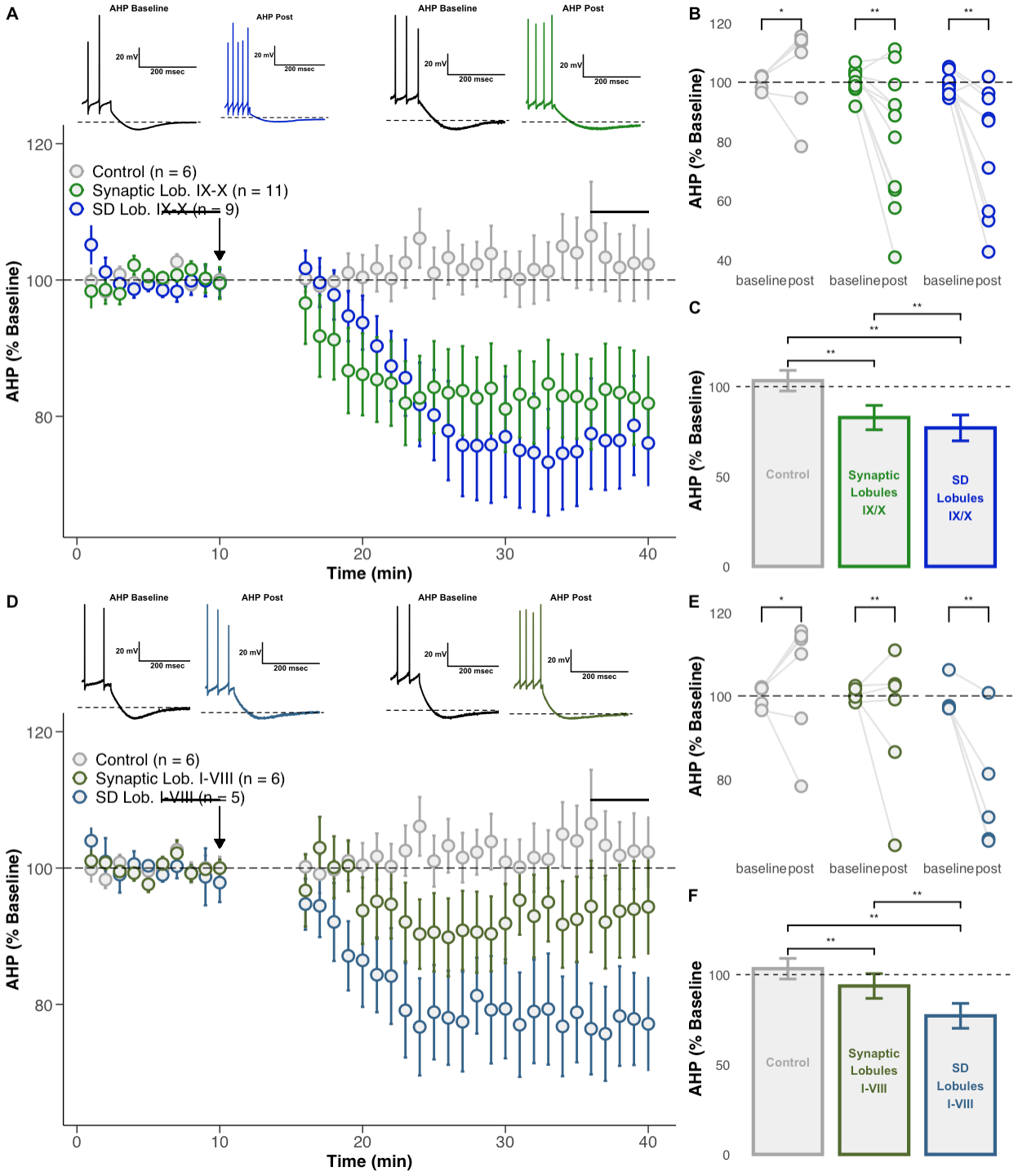

Figure 2.4 – AHP amplitude reduction accompanies changes in evoked firing during IP. ***A, D.*** Time series graph showing the minimum AHP amplitude as a percentage of baseline in response to SD and synaptic protocols. ***B, E.*** Change in AHP of individual cells. ***C, F.*** Average change in AHP. Data are presented as mean ± SEM. *Significance of $p<0.05$, **Significance of $p<0.01$.

2.4 EXPRESSION OF BOTH SYNAPTIC AND SD INDUCED INTRINSIC PLASTICITY IN PURKINJE CELLS IS DEPENDENT ON SK2 CHANNELS

As previously stated, the downregulation of SK2 channels is known to mediate neuronal excitability (Cingolani et al., 2002), and intrinsic plasticity induced by the SD protocol is absent in global SK2 knockouts (Grasselli et al., 2016). The question remains, however, whether these changes in excitability are due to Purkinje cell-specific SK2 channel activity. Additionally, it is not clear whether intrinsic plasticity induced by synaptic input also relies on SK2 channels. To address these questions, experiments were performed using L7-SK2 conditional knockout mice, which have a Purkinje cell-specific deletion of the SK2 channel.

For these experiments, recordings from across all lobules of the vermis were pooled because the rates of IP induction were not statistically different between lobules I-VIII versus lobules IX/X (Fig. 2.5 *B*, Mann-Whitney *U* test, $p = 0.55$; *D*, Mann-Whitney *U* test, $p = 0.42$). Consistent with the findings in Grasselli et al. (2016), the SD protocol failed to induce intrinsic plasticity in Purkinje cell-specific SK2 knockout mice (Fig. 2.6 *A-C* WT: 161.8 $\pm$ 11.1% baseline, paired Student's *t* test, p = 2.4 $\times$ 10^{-13}, n = 14; L7-SK2: 96.63 $\pm$ 10.3% baseline, paired Student's *t* test, $p = 0.24$, n = 6). When the synaptic LTP-burst protocol was applied, there was also no significant change in the evoked firing rate in Purkinje cells from conditioned animals. (2.6 *D-F* WT: 137.0 $\pm$ 10.7% baseline, paired Sutdet's *t* test $p = 3.9\times10^{-11}$, n = 17; L7-SK2: 104.7 $\pm$ 9.0% baseline, paired Student's *t* test, $p = 0.61$, n = 4).

Additionally, neither the SD nor the synaptic protocol led to a significant reduction in the AHP as observed in wild-type animals – and the SD protocol instead led to a small, but significant, increase in the minimum amplitude (Fig. 2.7 *B, E.* SD AHP: WT 77.0 $\pm$ 7.1% baseline, $p = 1.9\times10^{-12}$; L7-SK2 114.6 $\pm$ 3.7% basline, $p = 4\times10^{-4}$; Syn AHP: WT 88.2 $\pm$ 6.8% baseline, $p = 3.9\times10^{-11}$; L7-SK2 102.4 $\pm$ 5.8%baseline, $p = 0.61$; all statistics are paired Student's *t* test). Taken together, these results suggest that intrinsic plasticity, as measured by changes in both the evoked firing rate and AHP, is dependent on SK2 channel activity specifically in Purkinje cells.

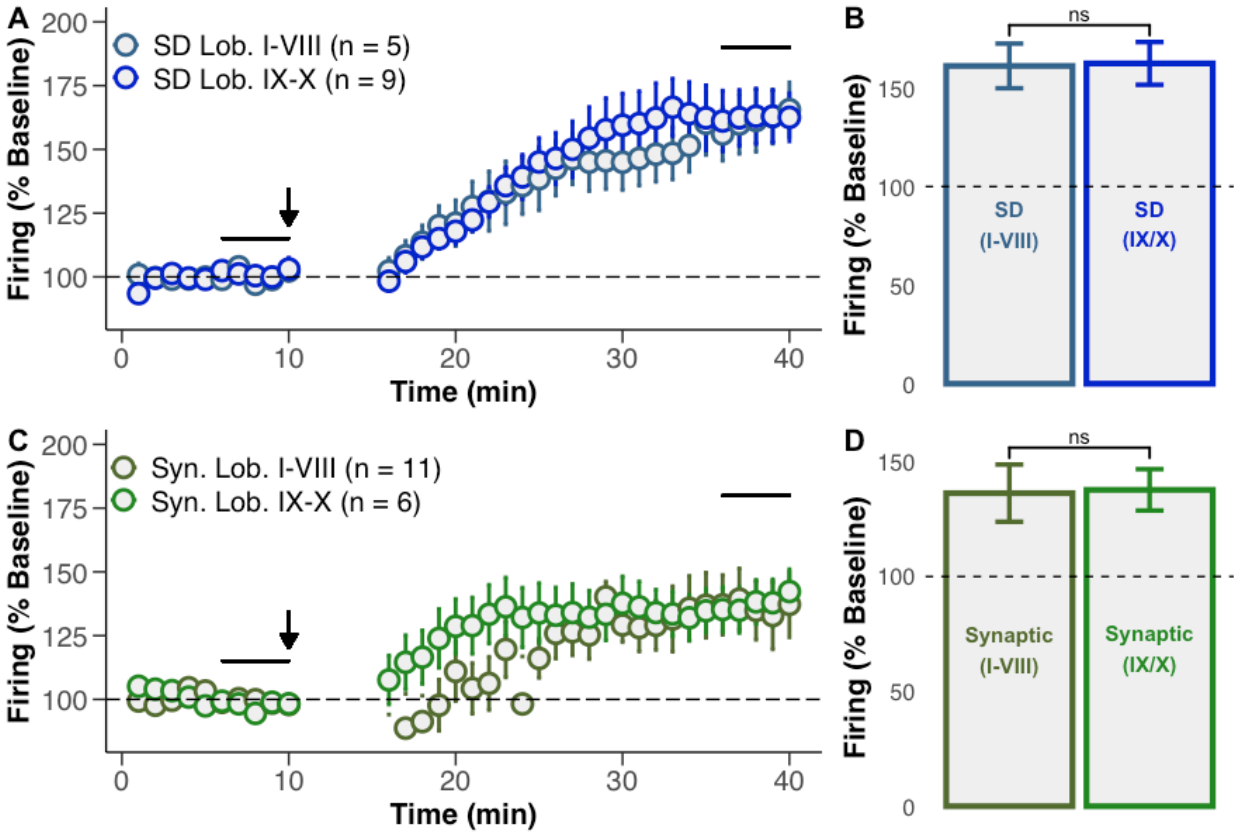

Figure 2.5 – The rate of intrinsic plasticity induced by either the synaptic or SD protocol is consistent throughout the cerebellar vermis. ***A, C.*** Time series plot showing the change in evoked firing relative to baseline in response to SD (top) and synaptic (bottom) induction protocols across all lobules of the cerebellum. ***B, D.*** Bar graph showing the mean change in evoked firing. Data are presented as mean ± SEM. *Significance of $p<0.05$.

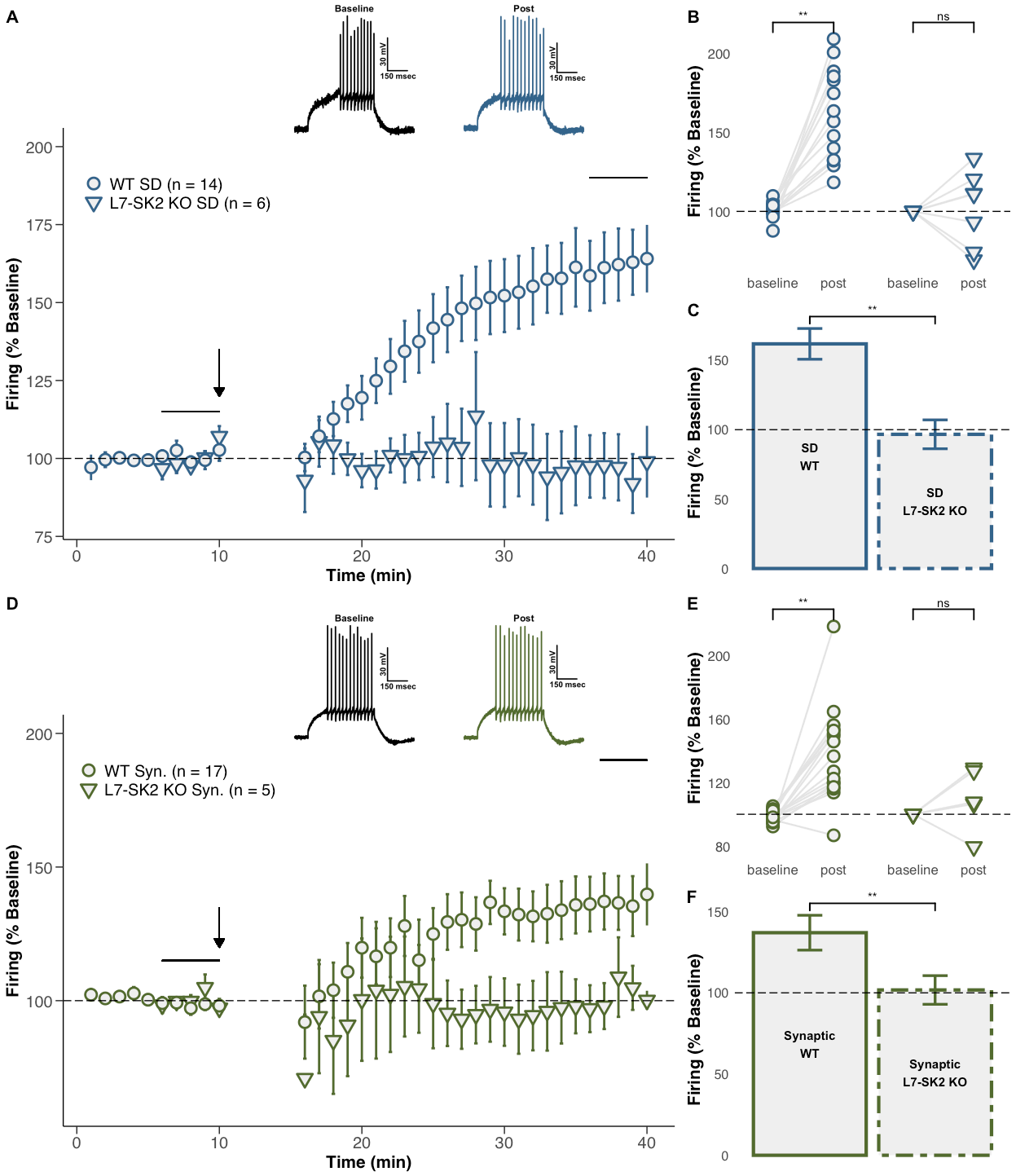

Figure 2.6 – Intrinsic Plasticity is blocked in Purkinje-cell specific SK2 knockouts. ***A, D.*** Time series plots showing the change in evoked firing relative to baseline in response to SD (top) and synaptic (bottom) input in WT (open circles) and PC-specific knockout mice (open triangles) across all lobules of the cerebellar vermis. ***B, E.*** Line plots showing the change in evoked firing of individual cells. ***C, F.*** Bar plot showing the mean change in evoked firing rate. Data are presented as mean ± SEM. *Significance of $p<0.05$.

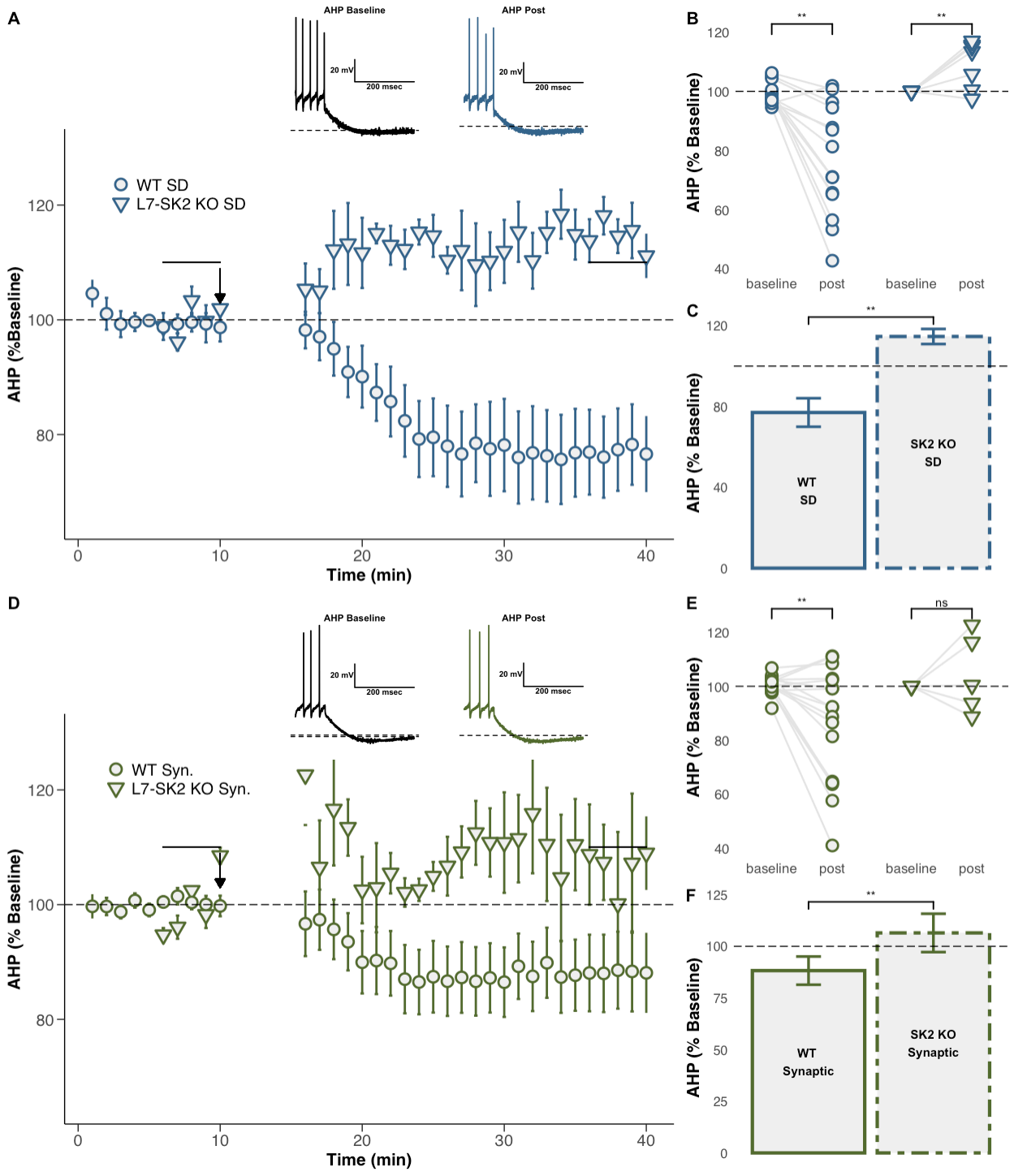

Figure 2.7 – AHP amplitude reduction is absent in Purkinje cell-specific SK2 knockouts. ***A, D.*** Time series graph showing the minimum AHP amplitude as a percentage of baseline in response to SD (top) and synaptic (bottom) protocols. ***B, E.*** Change in AHP of individual cells. ***C, F.*** Average change in AHP amplitude. Data are presented as mean ± SEM. *Significance of $p<0.05$.

2.5 METABOTROPIC RECEPTOR ACTIVITY MODULATES EXPRESSION OF INTRINSIC PLASTICITY

In the cerebellum, mAChRs are expressed in the vestibulocerebellum (lobules IX/X), which receives cholinergic afferents from the vestibular nuclei (Barmack et al., 1992; Jaarsma et al., 1997). Group I metabotropic glutamate receptors (mGluR), like mAChRs, activate the G_q signaling pathway; and mGluR1 is broadly expressed throughout the cerebellum.

In order to determine the effect of metabotropic receptor activation on cerebellar IP expression, recordings were performed in which a five minute bath application of either the general mAChR agonist oxotremorine-m (oxo-m; 7 μM) or mGluR1 agonist DHPG was delivered at the start of the induction protocol. For the SD experiments, this meant that the drug was still being added into the bath during the first 4 minutes of the post-induction recording period, while the post period for the synaptic protocol began with a return to ACSF; for both protocols, the drug was washed out bath by the last five minutes of the post period, as confirmed in Rinaldo and Hansel (2013).

In the absence of any stimulation, bath application of both oxo-m and DHPG caused a small but significant increase in the evoked firing rate of Purkinje cells (Fig. 2.8, oxo-m Ctrl. 109.1 $\pm$ 6.6% baseline, $p = 4.7\times10^{-5}$, n = 6; DHPG Ctrl. 112.8 $\pm$ 9.9% baseline, $p = 0.035$, n = 4; all stats paired Student's *t* test). Notably, while DHPG had a strong effect on the firing rate while it was in the bath, this effect was transient compared to the overall change in activity, and by the time the drug had washed out, there was not a significant difference detected in the change in firing rate evoked by either oxo-m or DHPG (Fig. 2.8 *B* Mann-Whitney *U* test, p = 0.55). Therefore, both oxo-m and DHPG are able to independently increase the firing rate of Purkinje cells through activation of metabotropic receptors. While the SD protocol was still able to generate an increase in the evoked firing rate after application of oxo-m and DHPG (Fig. 2.9 *B.* SD + oxo-m 161.3 $\pm$ 11.7% baseline, $p = 1.1\times10^{-5}$, n = 7; *F.* SD + DHPG 157.8 $\pm$ 14.1% baseline, $p = 2.6\times10^{-5}$, n = 5; all stats paired Student's *t* test), the presence of either drug in conjunction with the somatic depolarization protocol did not lead to a significantly different change in evoked activity when compared to use of the SD protocol alone (Fig. 2.9 *B.* SD IX vs. SD + oxo-m $p = 0.42$; *F.* SD

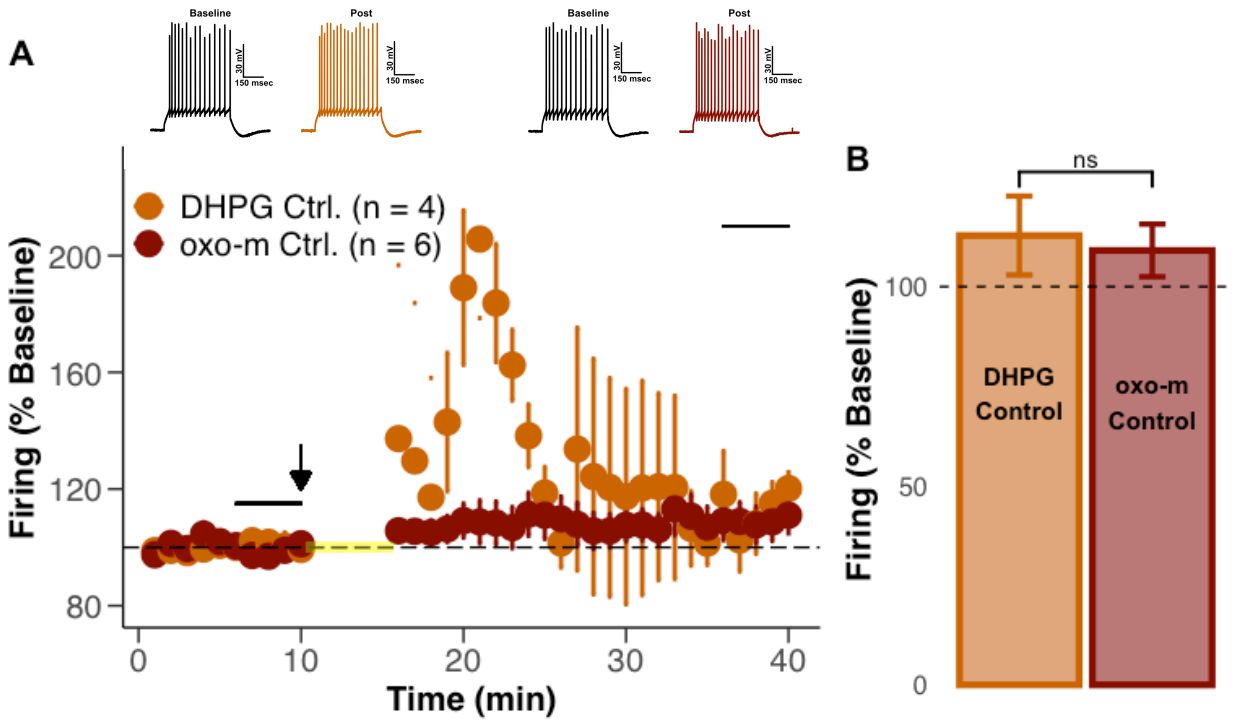

Figure 2.8 – Activation of metabotropic receptors increases evoked activity in the absence of stimulation. ***A.*** Time series plot showing the change in the evoked firing rate of Purkinje cells relative to baseline in response to bath application of either DHPG in cells from lobules I-VIII (orange) or to oxo-m in cells recorded from lobules IX/X in the absence of either SD or synaptic stimulation. ***B.*** Bar graph comparing the mean change in evoked firing of the groups in the time series plots to the left. Data are presented as mean ± SEM. *Significance of $p<0.05$.

I-VIII vs. SD + DHPG $p = 0.22$, all stats Mann-Whitney U test).

In contrast, when the synaptic protocol was applied in the presence of either oxo-m or DHPG, there was significant increase in evoked activity when compared to the change seen following synaptic stimulation alone (Fig. 2.10 Syn + oxo-m 177.4 ± 9.4% baseline, $p = 4.4\times10^{-6}$, paired Sutdent's t test, n = 9; Syn + DHPG 184.7 ± 19.8% baseline, $p = 2.7\times10^{-5}$, n = 5 ; Syn IX/X vs. Syn + oxo-m $p = 0.008$, Mann-Whitney U test; Syn I-VIII vs. Syn + DHPG $p = 0.008$, Mann-Whitney U test). In light of the fact that pharmacological metabotropic receptor activation is able to increase evoked activity in the absence of cellular input, it is important to determine whether the observed facilitation of synaptic-generated intrinsic plasticity is merely due to a summation of the two responses. In order to do this, the mean firing rate in response to oxo-m and DHPG was summed with the mean synaptic response in the corresponding lobules (ΣSynaptic + oxo-m

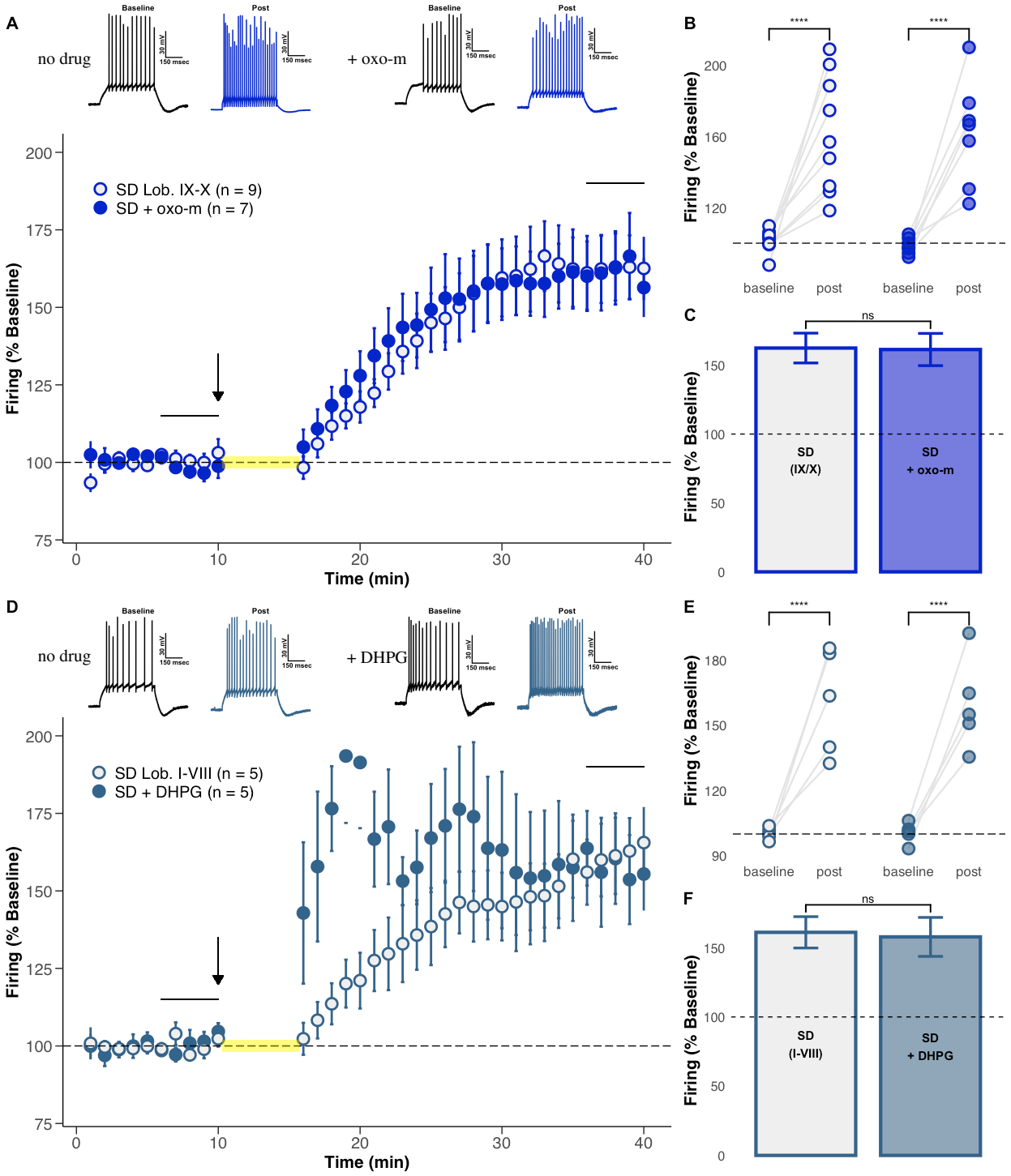

Figure 2.9 – Metabotropic receptor activity does not affect SD-induced intrinsic plasticity. ***A, D.*** Time series graph showing the change in evoked firing relative to baseline using the SD protocol in the presence of a region-specific metabotropic agonist in lobules IX-X (top), and lobules I-VIII (bottom). ***B, E.*** Change in evoked firing of individual cells. ***C, F.*** Bar graph depicting the mean change in evoked firing when the SD protocol is used alone vs. in the presence of a metabotropic agonist. Data are presented as mean ± SEM.

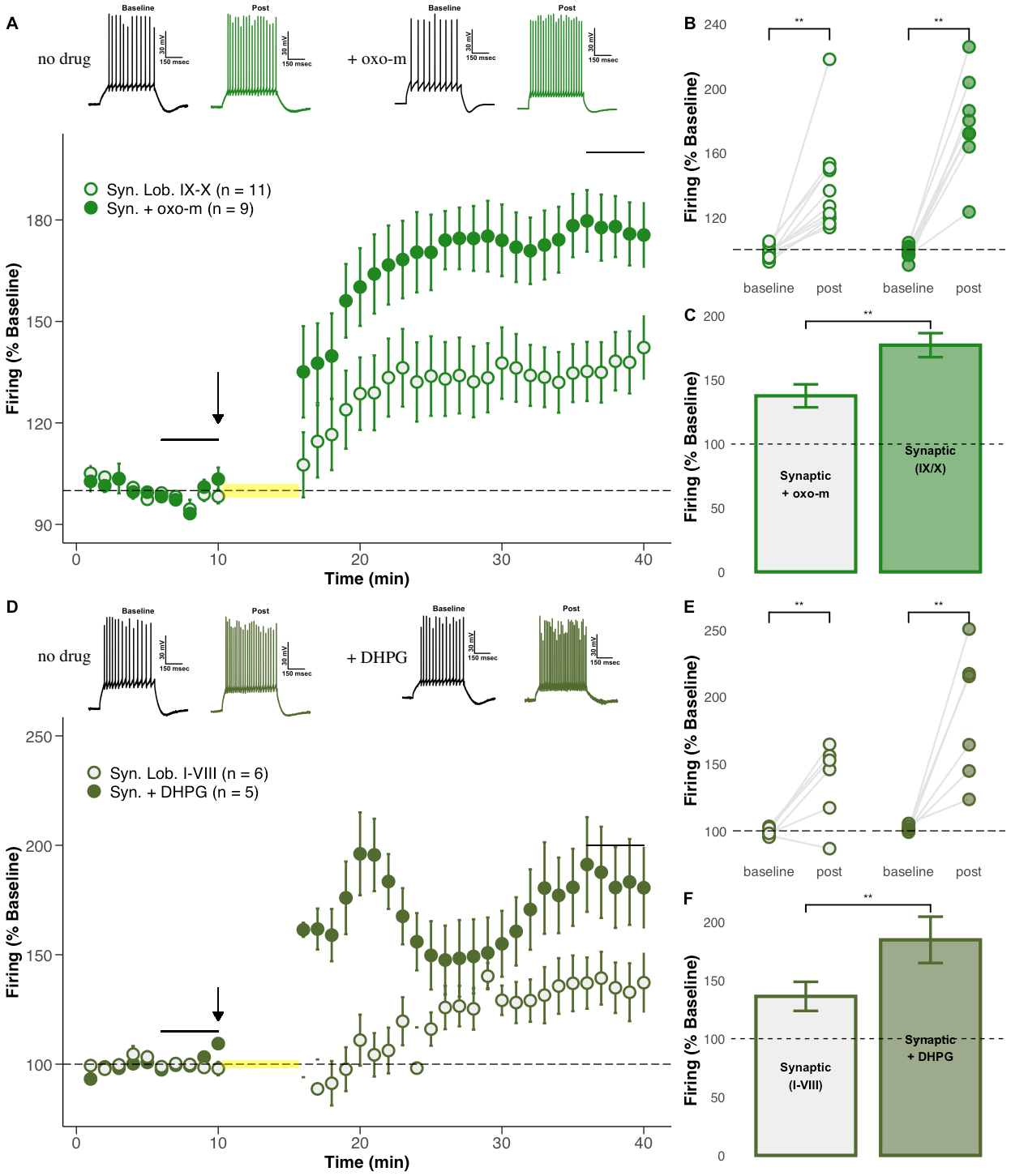

Figure 2.10 – Metabotropic receptor activity facilitates expression of synaptic-induced intrinsic plasticity. ***A, D.*** Time series graph showing the change in evoked firing relative to baseline when the synaptic protocol is used with with either oxo-m in lobules IX/X (top), or DHPG in lobules I-VIII (bottom). ***B, E.*** Change in evoked firing of individual cells. ***C, F.*** Bar plot comparing the mean average change in evoked firing of the groups shown in the time series plots to the left. Data are presented as mean ± SEM. *Significance of $p<0.05$, **Significance of $p<0.01$.

or ΣSynaptic + DHPG), and the variance was averaged. These values, in turn, were compared with the data recorded when the synaptic protocol was used with either oxo-m or DHPG. Based on this model, metabotropic receptor activation facilitates the Synaptic IP response to a greater extent than what would be predicted if the effect were purely additive (Fig. 2.11 *B.* ΣSynaptic + oxo-m vs. Synaptic + oxo-m $p = 2.2\times10^{-4}$; *D.* ΣSyn + DHPG vs. Syn + DHPG $p = 0.0071$; all stats Mann-Whitney *U* test).

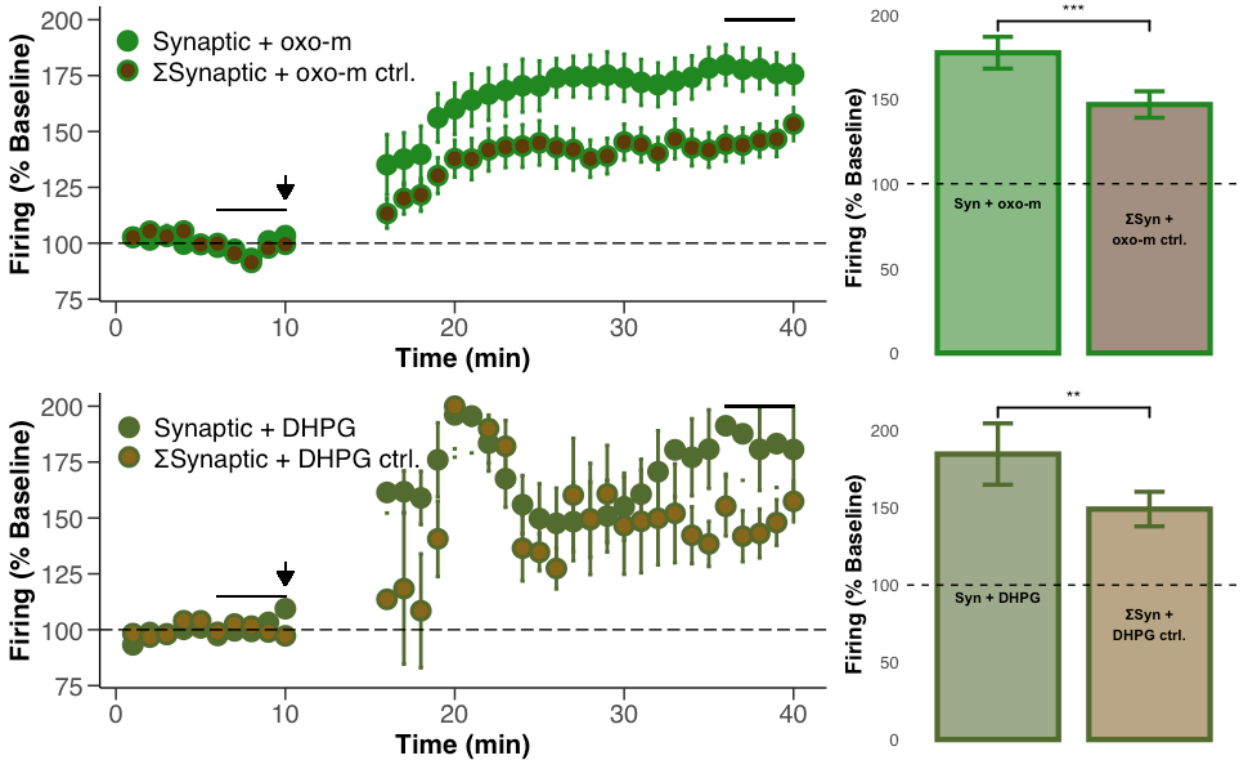

Figure 2.11 – Activation of metabotropic receptors facilitates IP induced by the synaptic protocol in a superlinear manner. ***A, C.*** Time series plot showing both the evoked firing rate as observed when the synaptic protocol was used along with bath application of either oxo-m in cells recorded from lobules IX/X (Synaptic + oxo-m), or of DHPG in lobules I-VIII (Synaptic + DHPG); along with the computed estimate of what the values would be if the mean synaptic response alone for each region were summed with either the mean response of the oxo-m control (ΣSynaptic + oxo-m) or DHPG control (ΣSynaptic + DHPG) groups. ***B, E.*** Bar plots comparing the mean average change in the evoked firing rates of the groups shown in the time series graphs to the left. Data are presented as mean ± SEM. *Significance of $p<0.05$.

In order to look at how cholinergic signaling modulates intrinsic plasticity, the general mAChR agonist oxo-m was used in recordings; however, mAChRs are not homogeneous. The group con-

sists of five subtypes (M1-M5) that have diverse expression patterns and function throughout the central and peripheral nervous systems. Functionally, these subtypes are separatated into two groups determined by the G-protein to which each receptor is coupled, with the M1, M3, and M5 subtypes preferentially coupled to the $G_{q/11}$ family, and the M2/M4 receptors coupled to the $G_{i/o}$ family (Thiele, 2013). In the cortex and the hippocampus, activity of the M1 subtype specifically has been shown to modulate learning and both synaptic and intrinsic plasticity (Buchanan et al., 2010; Galvin et al., 2020). The cerebellum primarily expresses the M1-M3 subtypes, and M3 activity has been shown to suppress LTP at the PF-PC synapse (Rinaldo and Hansel, 2013). In order to determine whether the observed cholinergic facilitation of intrinsic plasticity was subtype specific, recordings were performed with both oxo-m and either the M1-specific antagonist telenzepine (tzp) or the M3-specific antagonist DAU 5884 in the bath during the induction period.

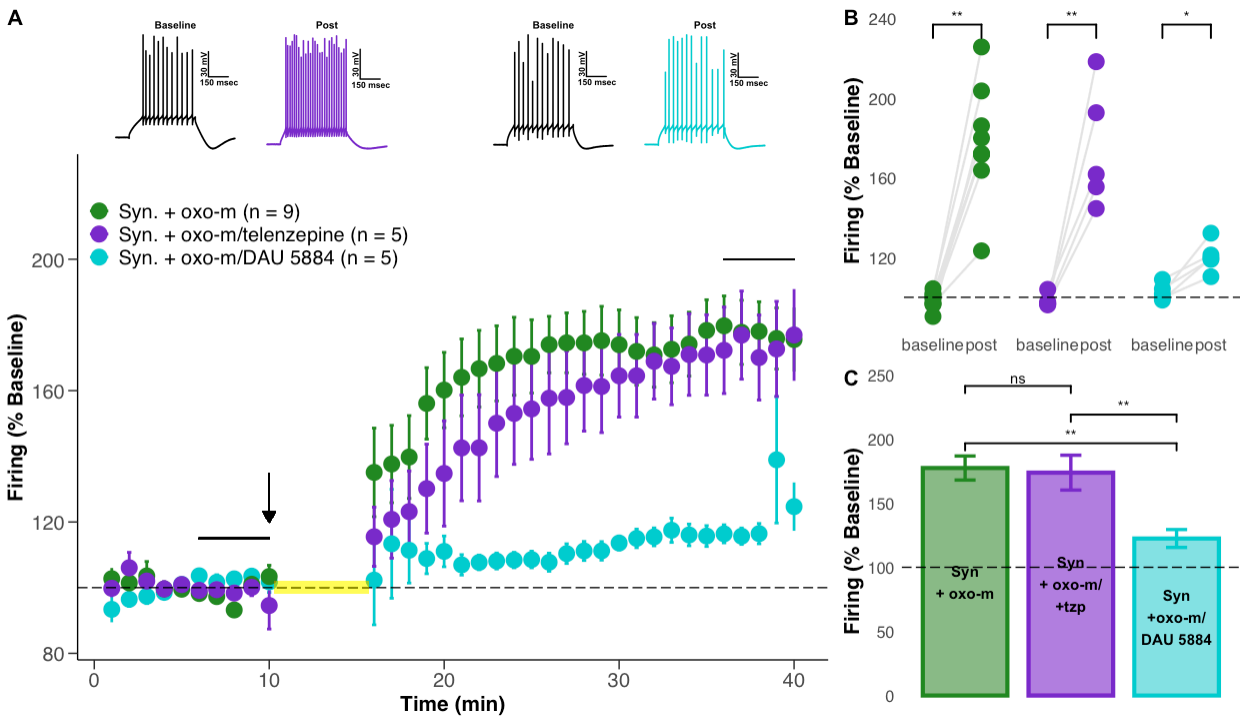

Figure 2.12 – The M3 subtype mediates facilitation of intrinsic plasticity. ***A.*** Time series graph showing the change in evoked firing relative to baseline when the synaptic protocol is used with either an M1 (purple) or M3 (teal) specific antagonist in conjunction with oxo-m. ***B.*** Change in evoked firing of individual cells. ***C.*** Bar graph depicting the mean change in evoked firing. Data are presented as mean ± SEM. *Significance of $p<0.05$, **Significance of $p<0.01$.

Using the synaptic protocol, which showed a clear effect of mAChR facilitation, there was a significant increase in evoked firing when blocking both M1 (173.8 $\pm$ 13.6% baseline, p = 0.01, paired Student's t test, n = 5) and M3 (122.4 $\pm$ 7.0% baseline, $p = 3.6\times10^{-6}$, paired Student's t test, n = 5) activity (Fig. 2.12 *A, B*). Although the increase in evoked activity was not absent when M3 activity was blocked, it was significantly reduced when compared to what was observed with either oxo-m alone or only M1 receptors blocked (DAU vs. oxo-m, p = 0.008; DAU vs. tzp p = 0.008, Mann-Whitney U test). By contrast, there was no significant difference detected in the facilitation of intrinsic plasticity observed when M1 activity alone was blocked in comparison to use of oxo-m alone (oxo-m vs. DAU p = 0.095, Mann-Whatney U test).

2.6 EXPRESSION OF INTRINSIC PLASTICITY IS MEDIATED BY PKA

In numerous regions of the brain, cholinergic activity has been shown to modulate SK channel activity, although there is not yet consensus on what mechanism precisely leads to this effect (Maylie and Adelman, 2010). As previously noted, Both the M1, M3, and M5 mAChR subtypes and mGluRs activate the G_q signaling cascade, and one of the downstream effects of this pathway is an increase in the activation of both PKC and PKA (Chen et al., 2017). Interestingly, PKA-dependent

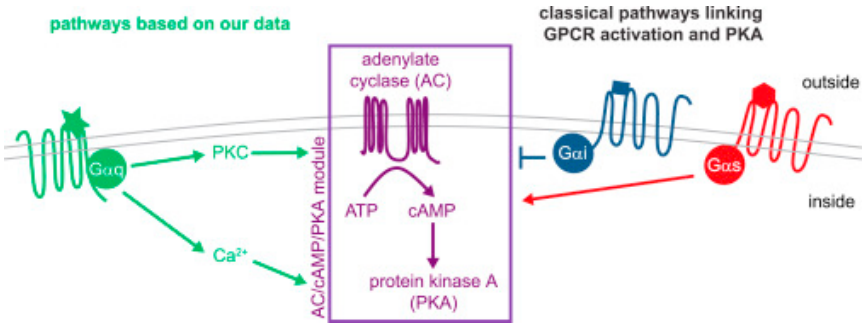

Figure 2.13 – Model of GPCR modulation of PKA activity. Adapted from Chen et al. (2017)

phosphorylation has been shown to be necessary for SK channel endocytosis, which leads to an increase in cellular excitability (Duffy and Nguyen, 2003; Ren et al., 2006); and in Purkinje cells, SK2 channels have been shown to associate with mGluR1α (Luján et al., 2018). Based on this information, experiments were performed to look at how pharmacological block of PKA activa-

tion via postsynaptic application of a PKA competetive inhibitor, Rp-cAMPS (cAMPS) through the recording pipette (Duffy and Nguyen, 2003) would affect expression of intrinsic plasticity in Purkinje cells (see Fig 2.13 for mechanism).

When PKA activation was inhibited by the peptide cAMPS, the SD protocol did not generate a change in evoked firing rate (Fig. 2.14 *A-C*, SD + cAMPS 103.3 ± 10.9% baseline, $p = 0.45$, paired Student's *t* test).

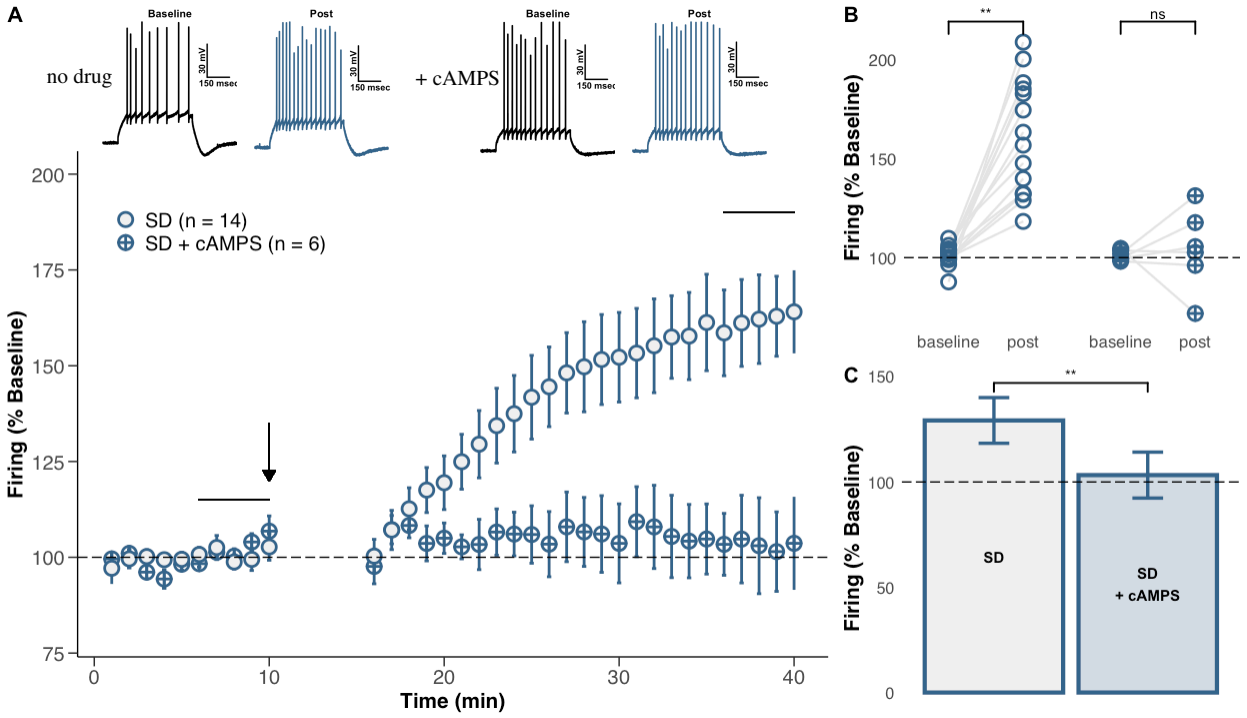

Figure 2.14 – Intrinsic plasticity is blocked in the absence of PKA signaling. ***A, D.*** Time series graphs showing the evoked firing rate of the SD protocol (top) and the synaptic protocol (bottom) across all lobules of the vermis, either alone (open circles) or in the presence of PKA inhibiting peptide cAMPS (cross-hatched circles). ***B, E.*** Line plots showing changes in the evoked firing rate of individual cells that contribute to the time series plots to the left. ***C, F.*** Bar graphs comparing the mean average change in the evoked firing rates of the groups shown in the time series graphs to the left. Data are presented as mean ± SEM. *Significance of $p<0.05$.

2.7 DISCUSSION

The current body of work looking into the molecular pathways that lead to induction and maintenance of intrinsic plasticity has relied on a range of induction protocols applied to a broad array of cell types in different regions of the brain. While the results of those experiments are useful in confirming the general occurrence of activity-induced changes in cellular activity, it is difficult to gain a more precise understanding of how this phenomenon occurs, and how its expression may be modulated under different contexts. The results presented here help clarify these questions.

Use of both the strong SD protocol and the more physiologically relevant synaptic protocol generated changes in the excitability of Purkinje cells – there was a significant increase in the evoked firing rate, as well as a significant reduction in the minimum amplitude following a depolarization step. Interestingly, the direct stimulation of the SD protocol generated a significantly stronger intrinsic plasticity response, which could have occurred due to a number of reasons. Firstly, because the SD protocol provides such strong stimulation to the cell, there could simply be a greater activation of the intracellular signaling pathways that generate the increases in firing rate and decrease in AHP. Alternatively, because recordings were made at the soma, these experiments may not have been picking up more local changes in SK channel expression at the synapse that may have been induced by the synaptic protocol. Given that the synaptic protocol both more closely mimics input that Purkinje cells would receive during a learning scenario, and also is known to generate LTP, it is important to follow up on the effects of this stimulation in particular.

SK channels are known to modulate both firing rate and AHP in many kinds of neurons; Purkinje cells, however, express only the SK2 isoform. When experiments were repeated in Purkinje cell-specific knockout mice, the previously observed change in evoked activity generated by both the SD and synaptic protocols was blocked. Both of these results are important: firstly because this is confirmation that physiologically relevant stimulation also relies on proper SK channel function, and the involvement of the channels is not due to an artifact of artificial stimulation; secondly, the lack of an intrinsic plasticity response in the conditional knockouts probably was not due solely to

insufficient stimulation, as both the synaptic protocol and the stronger SD protocol did not show changes in excitability.

The results of these experiments also confirm that the modulatory effects of cholinergic activity on intrinsic excitability observed in pyramidal cells in the cerebral cortex and the hippocampus are consistent, to a certain extent, in cerebellar Purkinje cells. Bath application of the general mAChR receptor agonist in the absence of either the synaptic or SD induction protocol was sufficient to induce a small but significant increase in the evoked firing rate (Fig. 2.8). Interestingly, facilitation of the increase in the evoked firing rate was only observed in response to the synaptic protocol. This could be due to the fact that that, because the SD protocol alone produced such a strong response, there was a sort of ceiling effect which blocked further increases in plasticity. Alternatively, stimulation of synaptic inputs in a behaviorally relevant way could have led to activation of further intracellular signaling pathways that worked in synergy to increase the firing rate. This view is supported by the fact that the effect of oxo-m activity during the synaptic induction protocol caused a superlinear facilitation of evoked firing.

Although the verification of the effects of cholinergic input in the cerebellum is important, mAChR activity is restricted to the vestibulocerebellum (lobules IX/X). Crucially, for the understanding of the basic mechanisms of IP function, these results were confirmed using application of DHPG, an mGluR1 agonist. mGluRs share a downstream signaling pathway with mAChRs, so these results suggest that the observed results are not dependent solely on the type of input cells receive, but convey information about the pathways that allow for expression of intrinsic plasticity more generally. Additionally, these results suggest that the whole cerebellum, and not just lobules IX/X, is capable of responding to experience-based activity in a similar way, and modifrying that expression through the G_q-signaling pathway.

In order to further dissect the intracellular pathways that lead to intrinsic plasticity, experiments were performed that used pharmacological blockade of PKA activity. Phosphorylation by PKA is known to contribute to synaptic plasticity, and has also been shown to facilitate forms of cortical and hippocampal learning. PKA phosphorylation is also necessary for SK channel downregulation,

and these experiments have confirmed that this is necessary for intrinsic plasticity. Additionally, PKA activity has been shown to be increased due to activation of G_q-coupled metabotropic receptors, such as mAChR and mGluR. Intracellular blockade of PKA, using the peptide cAMPs, over the entire timecourse of the experiment blocked expression of intrinsic plasticity through the SD protocol. As with the results of the SK2 conditional knockout experiments, this suggests that PKA activity is necessary for proper induction of intrinsic plasticity, and that the lack of a response is not due to a stimulation that is not strong enough.

CHAPTER 3

CEREBELLUM-DEPENDENT ASSOCIATIVE LEARNING INDUCES CHANGES IN PURKINJE CELL INTRINSIC EXCITABILITY

3.1 RATIONALE

Previous work on cerebellum-dependent learning has focused on the function of synaptic plasticity at Purkinje cell synapses, with particular emphasis on the role of LTD at the parallel fiber to Purkinje cell synapse. Recently, multiple forms of cerebellar learning have been associated with a variety of changes in intrinsic properties of neurons both in the cerebellum (e.g. Purkinje cells, Golgi cells), and neurons that are downstream targets of Purkinje cell input. Despite this wealth of data, it is not clear how intrinsic plasticity works with synaptic plasticity to give rise to cerebellum-dependent motor learning. To study this, these experiments focus on changes in the activity of Purkinje cells, the sole output neuron of the cerebellar circuit, in response to an associative learning task which is known to rely on neurons located within a particular microzone of the cerebellum.

3.2 MATERIALS & METHODS

Animals

All procedures were approved by and performed in accordance with the guidelines of the Animal Care and Use Committees of both Northwestern University and the University of Chicago. Experiments were performed using 5-8 week old male mice (C57BL/6J) obtained from Jackson Laboratory.

Surgery

Animals were anesthetized with 3-4% vaporized isoflurane mixed with oxygen at a flow rate of 1-2 liters/minute, with buprenorphine (0.052 mg/kg) given subcutaneously as an analgesic. Mice were placed in a stereotaxic device and a midline incision was made along the scalp. The skin was

retracted laterally and the periosteum was scraped away. Two small screws (one in front of Bregma and one in front of Lambda) were implanted into the skull left of the midline. A ground wire of a headpiece containing five wires (one ground, two shock-delivering, and two EMG recording wires) was wrapped around the screws in a figure eight pattern. A thin layer of adhesive cement was placed on the skull, the screws, and the wire. The skin around the right eye was retracted to reveal the muscle lateral to the eye. Two shock-delivering wires were placed under the skin, caudal to the right eye and two EMG recording wires were placed on the musculus orbicularis behind the eyelid. The headpiece was stabilized with dental cement. The base of the wires was stabilized with another layer of cement. The animal was allowed to recover on a warmed heating pad before being placed back in its home cage. Mice were allowed to recover one week after the surgery before beginning delay eye-blink conditioning training.

Delay eye-blink Conditioning

Animals were randomly assigned to one of three behavioral groups: naive, pseudoconditioned, or conditioned. The training apparatus consisted of a sound attenuating training chamber (IAC Acoustics) containing a cylindrical treadmill on which head fixed mice were able to freely run, (Lin et al., 2016). Mice were allowed to habituate to the chamber and cylindrical treadmill during two separate sessions the day before training (Training 0). During each habituation session, the mice were placed on the cylindrical treadmill for the same duration as one training session in the absence of stimuli presentation. One day after habituation, mice were trained for two sessions a day over the course of three days, with a two hour interval between training sessions. Conditioned mice received the delay eye-blink conditioning paradigm, which consisted of a 75 dB tone (350 ms, 2 kHz) conditioned stimulus (CS) paired with a 100 ms unconditioned stimulus (US) consisting of 6 sets of biphasic shocks (120 Hz; 1 ms/pulse) to the periorbital region using a biphasic stimulus isolator (WPI model A385). The US intensity was adjusted for each mouse to elicit a reliable blink (0.3-2 mA). The CS overlapped with and co-terminated with the US. Each training session consisted of 30 paired CS-US trials with a random 30-60 second inter-trial interval. Animals

in the pseudo conditioned group were presented with 30 unpaired CS trials and 30 unpaired US trials in pseudorandomized order with a 15-30 second inter-trial interval during a training session of the same length. Naive animals underwent surgery and habituation, and did not receive any presentation of stimuli during training sessions. EMG signals were amplified and filtered through 100 to 5 kHz low/high pass filter. The signals were rectified and integrated with a time constant of 10 ms. Baseline EMG activity was defined as the average activity 250 ms before CS onset. Conditioned responses were identified as having EMG activity 4 standard deviations above the baseline, present at least 20 ms before US onset. The electrophysiological experiments described below were performed with the experimenter blind to the training condition of each mouse.

Dissections & Slice Preparation

Within ~48 hours of the final delay eye-blink conditioning training session, animals were anesthetized with isoflurane and immediately decapitated. The cerebellum was removed and the right paravermis/hemisphere isolated in ACSF. $200\,\mu\mathrm{m}$ slices including lobule HVI were prepared with a Leica VT-1000S vibratome and incubated for at least 1 hr at room temperature in oxygenated ACSF.

Electrophysiology

Slices were continuously perfused with ACSF containing picrotoxin ($100\,\mu\mathrm{M}$, Sigma Aldrich) to block $\mathrm{GABA_A}$ receptors, and held at near-physiological temperature (32–$34\,^{\circ}\mathrm{C}$) over the course of the experiments. Slices were visualized using an x40 objective mounted on either a Zeiss Examiner A1 microscope or a Zeiss Axioskop2 FS plus microscope (Carl Zeiss MicroImaging). Patch-clamp recordings were made from Purkinje cells located at the base of the primary fissure. Currents were filtered at 3kHz, sampled at 20kHz, and acquired using Patchmaster software (HEKA Electronics). The access resistance was compensated (70-80%) in current clamp mode, and hyperpolarizing bias currents were applied to hold the membrane potential around -70 mV in all experiments except those measuring spontaneous activity. Cells were excluded if the bias current $>$1nA. Patch pipettes

(resistance 2–6 $\mathrm{M}\Omega$) were filled with internal solution.

Spontaneous activity was determined by measuring cell firing in current clamp mode over 1-second sweeps; Purkinje cells that did not generate action potentials with 0 pA injected current (i.e. no bias current) were excluded from experiments. Evoked activity was measured by holding Purkinje cells at -70 mV in current clamp mode and applying a 500 msec depolarization step that increased in 50 pA steps. Parallel fiber inputs were stimulated 10 times at 100Hz by placing a glass pipette filled with ACSF in the molecular layer around the distal dendrites of the Purkinje cell while held at -70 mV. The climbing fiber input was stimulated using an ACSF filled glass pipette placed in the granule cell layer below the targeted Purkinje cell.

Intrinsic plasticity was monitored during the test periods by injecting a 500 msec depolarizing current (300-800 pA) to evoke action potentials; during the baseline period, the variation in the number of evoked action potentials could not exceed $\pm 15\%$. The input resistance was monitored throughout the experiments by applying hyperpolarizing current steps (-100 pA) at the end of each sweep. During tetanization, depolarizing currents (100 mS) were injected at 5 Hz for 8 sec. Intrinsic plasticity recordings were excluded if the input resistance (R_i) or holding potential (V_h) changed by $\geq 15\%$ over the course of the baseline.

Data Analysis

CS and US were delivered and EMG signals were collected using custom software written for LabVIEW (National Instruments). Cellular data were analyzed using Excel (Microsoft), Igor (Wavemetrics), Statistica (Tibco) and RStudio(RStudio, PBC). All data are expressed as mean $\pm$ SEM. Statistical analyses were performed using the Mann-Whitney *U* test (between groups), paired Student's *t* test (within subjects), and two-way repeated-measures ANOVA tests as appropriate. Statistical comparisons were based on the number of cells recorded from. The number of mice used is indicated for each parameter tested.

3.3 MICE SUCCESSFULLY PERFORM A CEREBELLUM-DEPENDENT ASSOCIATIVE LEARNING TASK

Over the course of six consecutive training sessions, mice in the "conditioned" group – which were presented with an auditory tone (CS) that co-terminated with a periorbital shock (US) – were able to associate the two stimuli and successfully acquire a delay eye-blink conditioning response (Fig. 3.1, threshold criterion >80% CR). In contrast, animals in the "pseudoconditioned" group, which received unpaired CS/US trials, did not develop an eye-blink response (<20% CR during CS-only trials), and served as a control group. Changes in intrinsic membrane properties, synaptic responses, and excitability were measured approximately 48 hours following the final training trial to determine whether long-term intrinsic plasticity accompanies synaptic plasticity during cerebellar learning. All electrophysiology experiments and data analysis were performed blind to the training conditions of the animals.

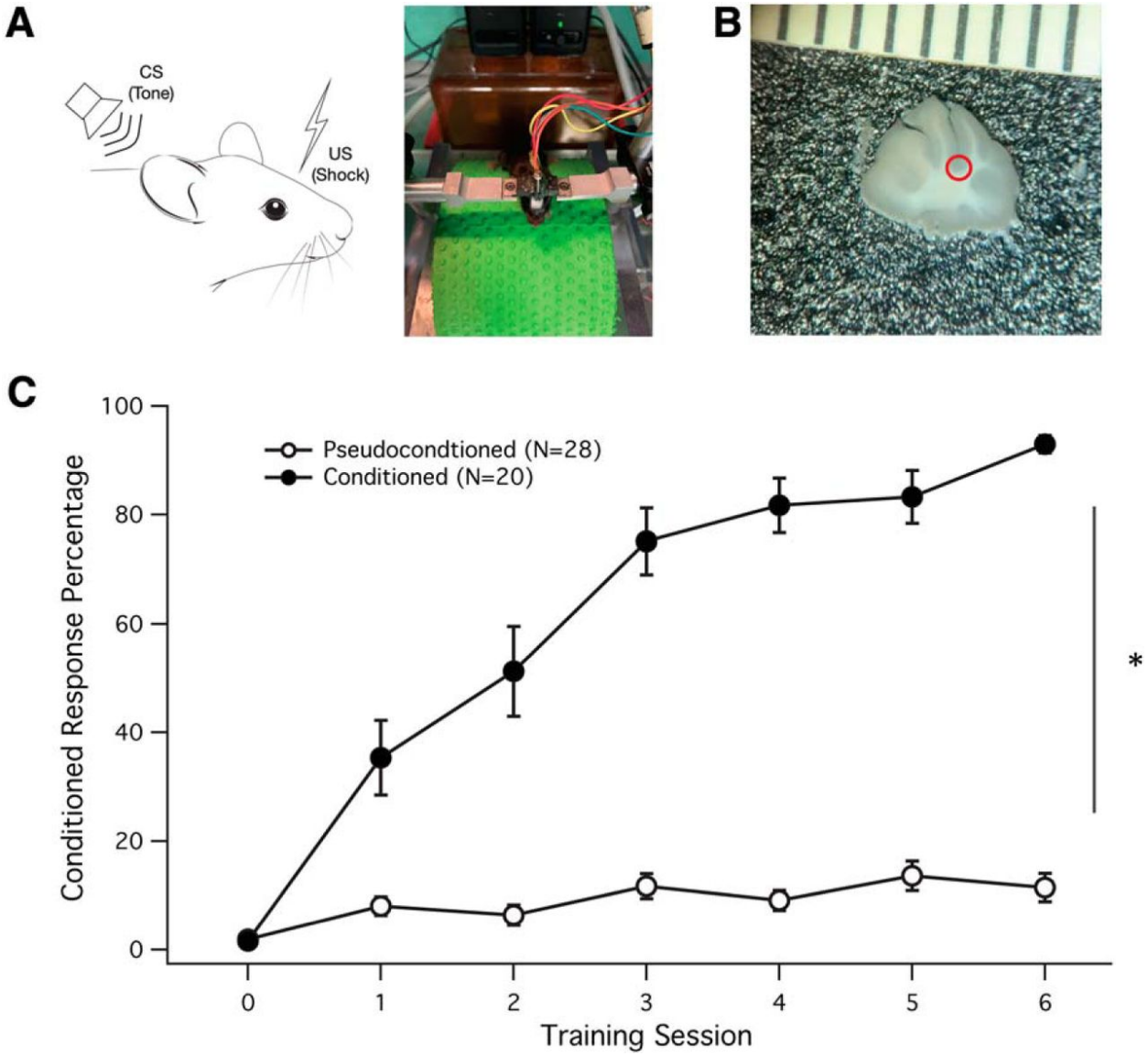

Figure 3.1 – Delay eye-blink conditioning generates learned behavior. ***A.*** Experimental setup. Left, Diagram of the CS (tone) and US (shock) stimuli applied to the test animal. Right, Original setup showing the mouse walking on a treadmill. ***B.*** Slice preparation illustrating the typical area at the base of the primary fissure from which patch-clamp recordings were obtained (red circle). The scale shows 1 mm units. ***C.*** Learning curve for conditioned (filled circles; N = 20), and pseudoconditioned mice (open circles, N = 28). Conditioned animals were successfully able to learn and generate a CR (eye closure) at a high percentage by the end of the 6th training session. Data are presented as mean ± SEM. *Significance of $p<0.05$.

3.4 SPONTANEOUS AND EVOKED SPIKING ACTIVITY IS NOT AFFECTED BY ASSOCIATIVE LEARNING

All cells recorded from were spontaneously active in the absence of bias current injection, and were monitored to ensure that they stayed healthy over the course of experiments. In order to determine whether associative cerebellar learning affects Purkinje cell activity, both spontaneous and evoked firing rates were measured under current-clamp conditions. Mice in the conditioned group did not display a significant difference in either the spontaneous or the evoked firing rate when compared with pseudoconditioned animals, nor was there a significant difference detected in the shape of the action potential waveform between the two groups.

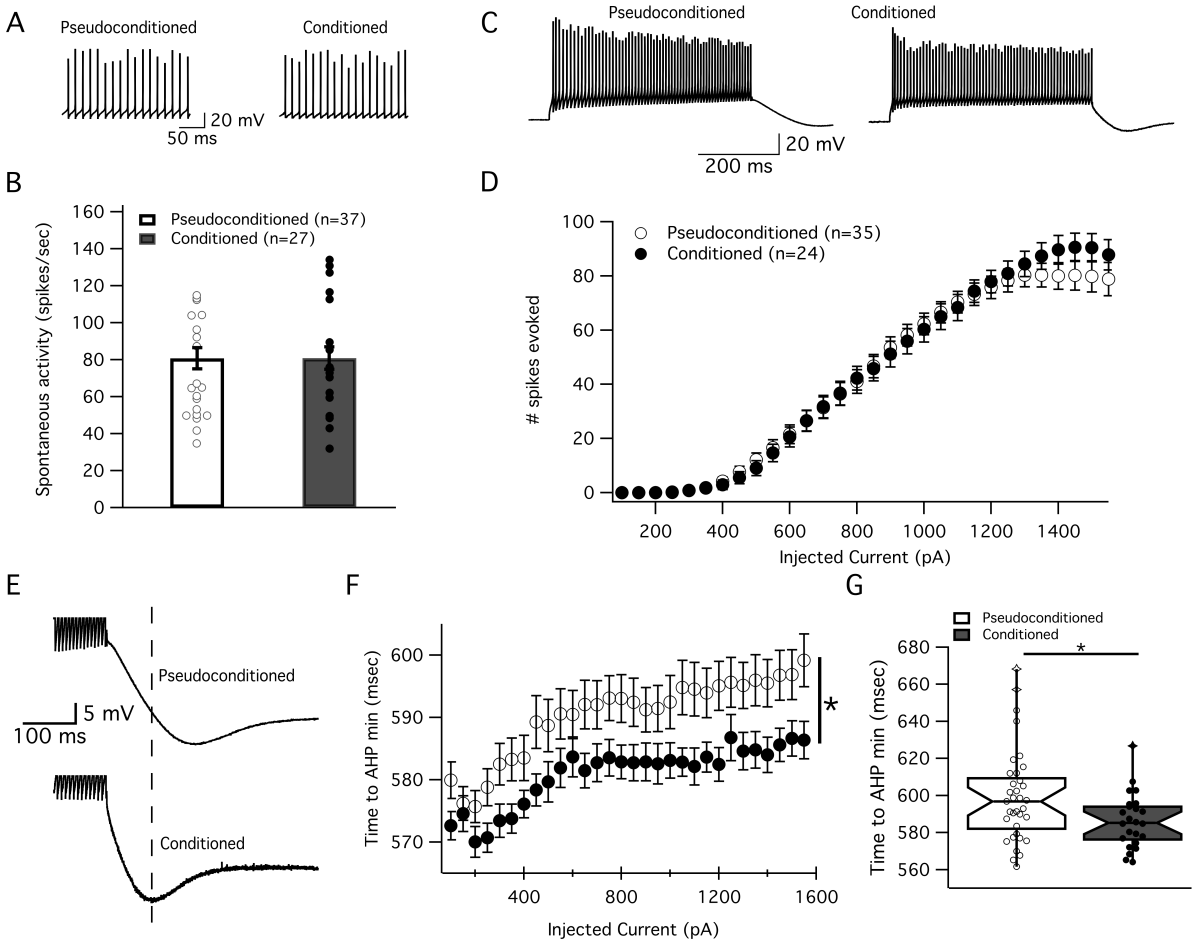

Figure 3.2 – Delay eye-blink conditioning has no effect on spontaneous or evoked spike firing in Purkinje cells. ***A.*** Example traces depicting spontaneous firing from Purkinje cells in a pseudoconditioned (left) and a conditioned (right) mouse. ***B.*** Spike count of action potentials per second measured from spontaneously firing cells (no bias current) from pseudoconditioned and conditioned mice. Dots represent individual cells, whereas bars represent the mean ± SEM. ***C.*** Example traces depicting evoked firing from cells in ***D.*** with 1550 pA current injected. ***D.*** Mean evoked firing (number of spikes) from pseudoconditioned (open circles) and conditioned (filled circles) over a series of injected currents. ***E.*** Example traces showing differences in the AHP between pseudoconditioned (top) and conditioned (bottom) mice. Dashed line indicates the timing of the AHP minimum for the trace obtained from a conditioned mouse. ***F.*** Timing of the AHP minimum amplitude as a function of injected current for pseudoconditioned (open circles) and conditioned (filled circles) mice. ***G.*** The mean time to the AHP minimum at 1550 pA injected current in pseudoconditioned and conditioned mice (taken from F). Data are presented as mean ± SEM. *Significance of $p<0.05$.

3.5 CONDITIONED ANIMALS DEMONSTRATE A REDUCTION IN AHP

During the measurement of evoked activity, both the firing rate and the mAHP, which is mediated in part by SK2 channels (Grasselli et al., 2016), were recorded at a regular series of current injection steps. Although no difference was detected between the two groups in the number of action potentials evoked, the time required to reach the minimum value of the AHP following the end of depolarization was significantly reduced in conditioned animals (Fig. 3.2; cond: 586.4 $\pm$ 3.0 msec, n=24, N = 14; pseudo: 599.2 $\pm$ 4.2 msec, n = 35, N = 18; at 1550 pA injected current; Mann-Whitney U test, p = 0.02). In order to determine whether this change in excitability is also present in response to less artificial stimuli, the AHP was also measured during responses to stimulation of both parallel fibers and climbing fibers, the two sources of excitatory synaptic input Purkinje cells receive.

Previous work has shown that during delay eye-blink conditioning, Purkinje cells undergo LTD at the PC-PF synapse. Under current clamp conditions, no significant differences were measured in either the depolarization envelope or firing rate between the two training groups in response to a 10x100 Hz stimulus. When the AHP was measured, however, conditioned animals demonstrated a significant decrease in the AHP relative to pseudoconditioned controls (Fig. 3.3). The minimum amplitude of the AHP was significantly reduced following associative learning (cond: -4.8 $\pm$ 0.4 mV, n=16, N = 14; pseudo: -6.0 $\pm$ 0.4 mV, n = 20, N = 18; Mann-Whitney U test, p = 0.03). Additionally, the area of the AHP (cond: -416.0 $\pm$ 51.1 msec*mV; pseudo: -747.6 $\pm$ 35.7 msec*mV; Mann-Whitney U test, p = 0.0006) and the overall duration (cond: 231.5 $\pm$ 17.5 msec; pseudo: 317.2 $\pm$ 26.6 msec; Mann-Whitney U test, p = 0.005) were significantly decreased in conditioned animals.

Purkinje cells produce a large excitatory response to climbing fiber input characterized by the all-or-none generation of a complex spike, which consists of a large Na^+ spike, followed by a number of smaller spikelets. In accordance with the change seen in response to PF burst stimulation, Purkinje cells from mice that successfully acquired the eye-blink response exhibited a significant increase in excitability (Fig. 3.4). Although no difference was detected in the minimum AHP

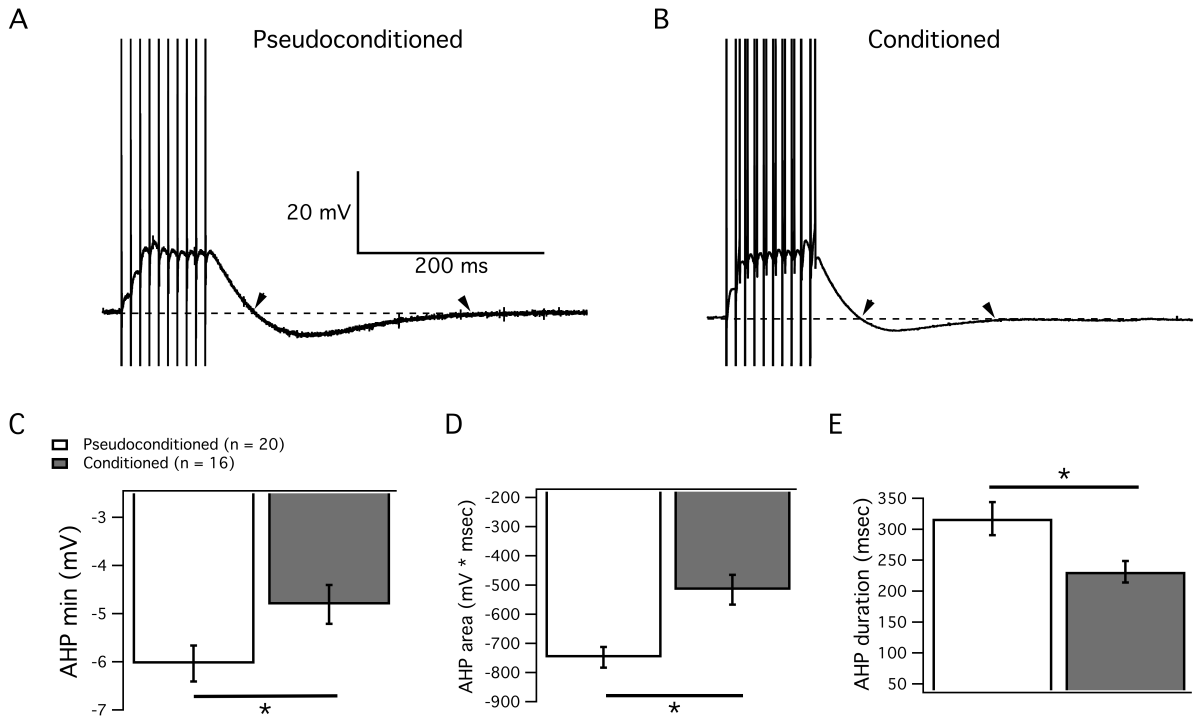

Figure 3.3 – Eye-blink conditioning reduces the AHP following PF burst stimulation. ***A,B.*** Example traces of the reponse to 10 parallel fiber stimuli at 100 Hz from cells from a pseudoconditioned (***A***) and a conditioned (***B***) mouse. Dashed line indicates the baseline potential at -70 mV. Arrowheads indicate the start and finish of the AHP. ***C-E*** Measures of the AHP after the PF burst in cells from pseudoconditioned (white) and conditioned (gray) mice. ***C.*** Minimum AHP amplitude. ***D.*** AHP area as measured between curve and baseline. ***E.*** Duration of the AHP. Data are presented as mean $\pm$ SEM. *Significance of $p<0.05$.

amplitude between the two training groups, there was a significant reduction in both the duration (cond: 210.0 $\pm$ 9.2 msec, n = 20, N = 17; pseudo: 280.5 $\pm$ 18.1 msec, n = 23, N = 17; Mann-Whitney *U* test, $p = 0.0019$) and the area (cond: -282.4 $\pm$ 15.0 msec*mV; pseudo: -385.6 $\pm$ 21.1 msec*mV; Mann-Whitney *U* test, $p = 0.0004$)of the AHP following CF stimulation. Additionally, the number of spikelets generated in the complex spike waveform was significantly increased following associative learning (cond: 2.19 $\pm$ 0.11; pseudo: 1.78 $\pm$ 0.15; Mann-Whitney *U* test, p = 0.042).

The observed reduction in post-firing AHP subsequent to both evoked activity and synaptic input is consistent with a downregulation of SK2 channels in Purkinje cells as a result of eye-blink

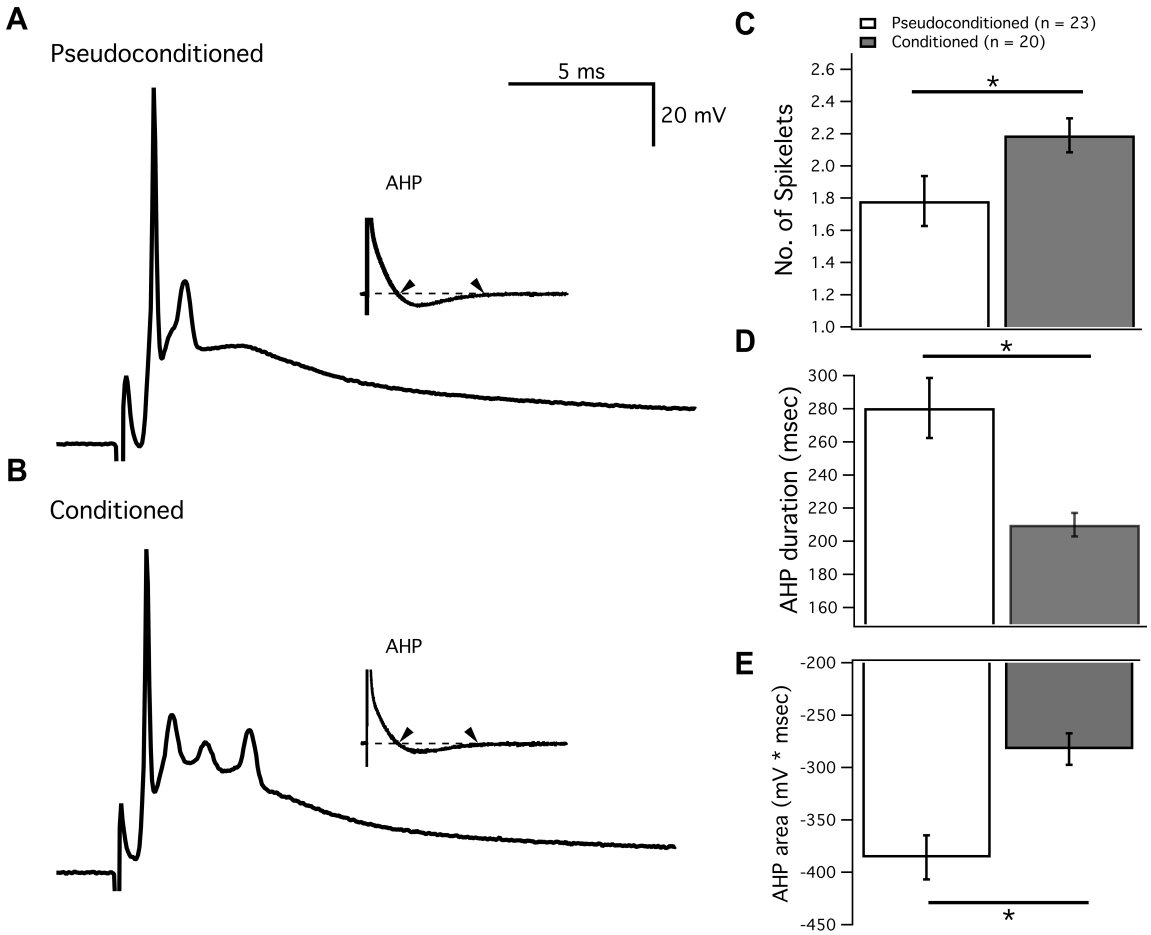

Figure 3.4 – Eye-blink conditioning alters the complex spike waveform. ***A,B.*** Example traces of complex spikes recorded from Purkinje cells in pseudoconditioned (***A***) and conditioned (***B***) mice. The insets show the waveform expanded to included the AHP. ***C.*** Bar graph showing the number of spikelets following the initial Na^+ spike. ***D,E.*** Measures of the AHP from pseudocondtioned (white) and conditioned (gray) mice. ***D*** AHP Duration. ***E*** AHP Area. Data are presented as mean $\pm$ SEM. *Significance of $p<0.05$.

conditioning.

3.6 INTRINSIC PLASTICITY EXPRESSION IS OCCLUDED IN CELLS FROM CONDITIONED MICE

In order to further test the relation between eye-blink conditioning and changes in neuronal excitability, Purkinje cells were repeatedly depolarized (5 Hz, 8s) using a tetanization protocol known to induce intrinsic plasticity (Belmeguenai et al., 2010). Subsequently, Purkinje cells from pseudoconditioned mice showed a significant increase in the number of evoked action potentials when compared with baseline activity (Fig. 3.5; paired Student's t test, p = 0.002); this change was absent in cells from conditioned animals (paired Student's t test, p = 0.63). The increased firing rate in cells from pseudoconditioned mice persisted at least 25 minutes following tetanization, and remained significantly higher than the firing rate of cells from conditioned animals measured during the same time period (pseudo. 143.3 $\pm$ 11.2%, n = 12, N = 10; cond, 113.1 $\pm$ 6.3%, n = 11, N = 10; Mann-Whitney U test, $p = 9.99 \times 10^{-7}$; 21-25 min. post induction). These results show that Purkinje cells from mice that successfully acquired a cerebellum-dependent associative learning task failed to show significant intrinsic potentiation following an IP induction protocol; whereas those from pseudoconditioned animals were able to increase excitability, suggesting that this form of intrinsic plasticity was occluded following delay eye-blink conditioning.

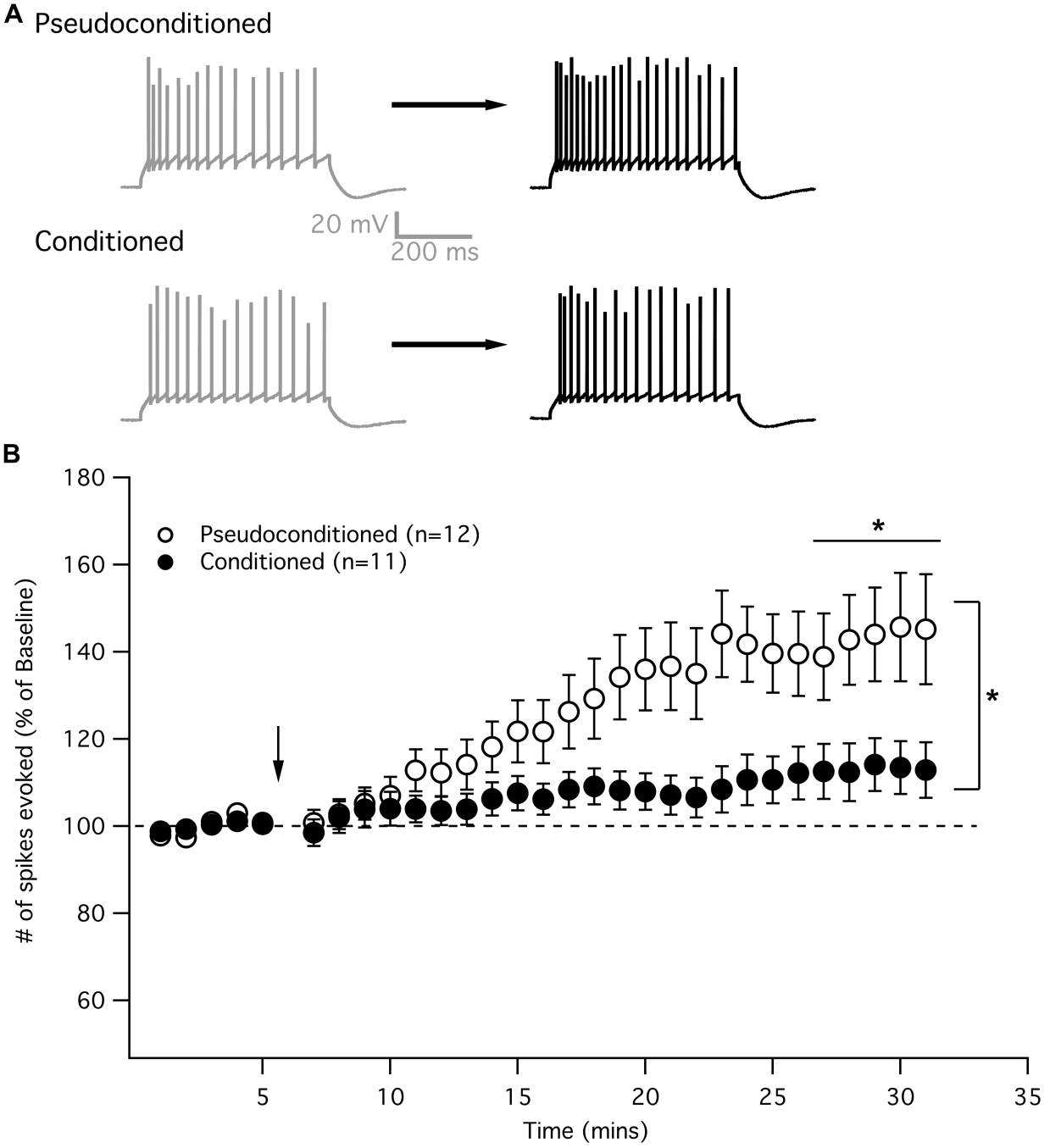

Figure 3.5 – Intrinsic plasticity is occluded in Purkinje cells from conditioned animals. ***A.*** Example traces of evoked activity during the baseline (gray) and following tetanization (black) in cells from pseudoconditioned (top) and conditioned (bottom) mice. ***A.*** Time series graph showing intrinsic plasticity (increase in evoked spiking as a percentage of baseline) in cells from pseudoconditioned (empty circles) and conditioned (filled circles) mice. Data are presented as mean ± SEM. *Significance of $p<0.05$.

3.7 DISCUSSION

Previous work in the hippocampus in rabbits had shown that the AHP amplitude is reduced following trace eye-blink conditioning in both CA1 and CA3 pyramidal neurons. (Moyer et al., 1996; Thompson et al., 1996) Similarly, and again in rabbits, Schreurs and colleagues observed a reduction in the AHP of Purkinje cells following a delay eye-blink conditioning task. Their study concluded that Purkinje cells in area HVI of conditioned mice showed a decrease in the dendritic spike threshold, as well as a reduction of the AHP following depolarization steps that can persist at least one month following the final training session (Schreurs et al., 1998; **?**).

The results presented here are consistent with and build upon these prior conclusions by showing a reduction in AHP measurements following not only depolarizing current injections (Fig. 3.2), but also in response to synaptic inputs (Fig. 3.3, 3.4). This suggests that regardless of the stiumuls driving calcium influx and ultimately, the AHP, training affects the kinetics and/or amplitude this event. The AHP is known to be involved in regulating the firing frequency of neurons, and in Purkinje cells, the AHP is known to be partially mediated by SK2 conductances, suggesting that SK2 channels might be downregulated during a delay eye-blink conditioning task. In a previous study, learning-related changes in the membrane excitability of Purkinje cells have been attributed to changes in A-type K^+-channels, as the effects on the dendritic spike threshold and the AHP could be mimicked by bath application of the I_A antagonist 4-AP (Schreurs et al., 1998); however, other research has shown that the presence of 4-AP does not occlude intrinsic plasticity (as measured by change in firing rate) triggered by repeated injection of depolarizing current pulses (**?**). Although it is possible that the differences in these observed results could be explained by the use of dendritic (Schreurs et al., 1998) as opposed to somatic (**?**) recordings, prior work using on dendritic recordings has confirmed a role for SK2 channels in Purkinje cell intrinsic plasticity, and observed that the phenomenon is absent in SK2 knockout mice (**?**). Nevertheless, as these experiments did not look specifically at the role of A-type K^+-channels, it cannot be ruled out that they also contribute to the expression of intrinsic plasticity in Purkinje cells.

The recordings for these experiments were performed in Purkinje cells located at the base

of the primary fissure in lobule HVI. This area has been identified as a microzone necessary for eye-blink conditioning in mice, and corresponds with the eye-blink microzone located in rabbits (**?**). That Schreurs et al. (1998) observed similar changes in Purkinje cells located more dorsally in HVI suggests that changes in excitability are not solely restricted to Purkinje cells at the core of the microzone, but could also occur in Purkinje cells in neighboring areas of HVI that may process both CS- and US-related information and contribute to the associative learning engram. The idea that more of HVI may be involved in eye-blink condition is supported by the observation of increases in the activity levels of PKC throughout the lobule, particularly in the dorsal region (Schreurs, 2019; **?**). Although it could not be confirmed that the Purkinje cells from conditioned animals used in recordings for these experiments were directly involved in the learning engram, the conclusions from the data remain relevant because the small size of the microzone makes it likely that at least some cells involved in the learned response were included; and also the results are consistent across the population of neurons.

Of particular interest was the finding that, following successful acquisition of associative learning, intrinsic plasticity is occluded in Purkinje cells from conditioned animals, while cells from pseudoconditioned mice remained able to increase their firing rate. Potentiation of the evoked firing rate relies on SK2 channels, and is absent both in the presence of the SK2 inhibitor apamin, as well as in mice lacking SK2 channel expression (Grasselli et al., 2016). Taken together with the decrease in mAHP seen in response to both synaptic and evoked input, this further suggests that intrinsic plasticity in the cerebellum converges on a decrease in SK2 channels; and that this form of learning is a key component of learning akin to synaptic plasticity (Titley et al., 2017).

CHAPTER 4

GENERAL DISCUSSION

Learning is characterized by on organism's ability to appropriately process and encode stimuli in order to adapt reflexes, make associations between inputs, and respond to environmental cues. Understanding the cellular and molecular processes that allow for appropriate learning are crucial not only to understand basic neural function, but also to understand what, precisely, can be done to alleviate pathologies that arise from abnormal learning.

To this end, the cerebellum has proven a useful model, due to both its highly organized and accessible structure, and its clearly defined function coordinating motor behavior. While much research has focused on how synaptic plasticity, particularly, at the parallel fiber-Purkinje cell synapse, affects cerebellum-dependent learning, it is less well established how experience dependent changes in the cell intrinsic properties of Purkinje cells – the principle cell of the cerebellar circuit – might contribute. The conclusions presented in the experiments that make up this dissertation aim to contribute to the broad field of learning-related research in two ways: First of all, by adding to the growing experimental support for the neurocentric model of learning, which posits that coordinated interaction between synaptic and intrinsic methods of plasticity are necessary for appropriate learning; and secondly, by investigating how intrinsic plasticity contributes to cerebellum-dependent learning in particular.

Although hopefully this work is conducive to providing at least moderately more insight into both intrinsic plasticity and cerebellar learning, it goes without saying that there are follow-up experiments based on questions raised by the results of these experiments that could and should be done to help further understand this area of research.

4.1 INTRINSIC AND SYNAPTIC PLASTICITY ARE INDUCED UNDER SIMILAR CONDITIONS

One of the main objectives of the work presented in this dissertation is to further emphasize how intrinsic plasticity functions in a complementary manner with synaptic plasticity, and how the two processes can be induced and modulated through parallel signaling pathways. In Chapter 2, it was shown that use of a synaptic protocol known to generate synaptic plasticity at the PF-PC synapse also leads to expression of intrinsic plasticity – specifically measured by an increase in the evoked firing rate, and a decrease in the minimum AHP amplitude. In Chapter 3, a similar reduction of the AHP was observed in conditioned animals that successfully acquired a cerebellar associative-learning task known to require synaptic plasticity.

The results in Chapter 2 also show that pharmacological and genetic manipulations *in vivo* that affect forms of learning known to require synaptic plasticity also have a corresponding effect on expression of intrinsic plasticity *in vitro*. SK channel activity has been shown to mediate both AP firing, and the mAHP of neurons. In the hippocampus and the cortex, it has been reported that blocking downregulation of SK channels impairs both LTP and behavior. The results presented in Chapter 2 show that Purkinje cell-specific elimination SK2 channels also leads to elimination of IP induction via use of the synaptic stimulation protocol.

Additionally, activation of mAChRs has been shown to facilitate both the expression of LTP and, as well as the acquisition and retrieval of memory in the hippocampus. The results in Chapter 2 show that mAChR activity during induction of the synaptic protocol also leads to a significant facilitation of the intrinsic plasticity response; that this facilitation is absent when mAChRs are activated during the synaptic protocol points to the conclusion that this particular modulation requires activity similar to what would be generated during behavior, and suggests that the downstream effects of this pathway are particularly important for understanding the interactions between synaptic and intrinsic plasticity. That a similar pattern of activity was observed when using a DHPG, a metabotropic agonist that activates a different receptor (mGluR) with a conserved downstream pathway (G_q-signaling) also emphasizes this point.

Further evidence that synaptic and intrinsic plasticity arise and function in concert comes from the PKA experiments in Chapter 2. Again, experiments in the hippocampus and cerebral cortex have established that enhanced PKA activation facilitates both synaptic plasticity and associated forms of learning; while inhibition impairs both. When PKA activation was blocked intracellular over the course of experiments, expression of intrinsic plasticity was also blocked in Purkinje cells.

That the same manipulations generate both changes in synaptic weights and excitability of single cells suggest that both synaptic and intrinsic plasticity are responding to similar inputs, such as what a cell would experience during learning. It therefore makes sense that the different responses of the two processes would cooperate to allow a single cell to participate in encoding a learned experience.

4.2 INTRINSIC PLASTICITY CONTRIBUTES TO CEREBELLAR LEARNING

The experiments described previously were also performed to understand more about how intrinsic plasticity might be involved in cerebellum-specific forms of learning. Although the circuitry of the cerebellum is well understood and the structure is relatively uniform, the input and output connectivity is not homogenous, and therefore not all areas contribute to all forms of learning. The cerebellum has been described as being organized into "microzones", which take part in specific aspects of motor learning. With this in mind, it is important to determine whether any observed learning-induced changes are a generalized component of cerebellar learning (i.e. the importance of LTD at the parallel fiber-Purkinje cell synapse); or a unique feature of a particular microzone (i.e. the different timing rules required to generate LTD in different regions of the flocculus (Suvrathan et al., 2018)). Taking the results of the experiments in Chapters 2 and 3 together suggests that induction of intrinsic plasticity contributes to cerebellar learning in a general fashion. The experiments in Chapter 2 were all performed in the vermis, which is centrally located and contains many microzones with different baseline levels of excitability. Conversely, the experiments in Chapter 3 were performed in a very specific region of the cerebellum, at the base of lobule HVI, which is known to be required for acquisition of the delay-eyeblink response in particular. Despite

the variation in regions, both learning (Chapter 3) and use of a synaptic protocol known to generate LTP (Chapter 2) led to significant changes in the intrinsic plasticity of Purkinje cells. One of the observed changes in excitability was a reduction in the mAHP, which is mediated by SK2 channels. This was seen in recordings taken from both the vermis and hemisphere, suggesting that not only is intrinsic plasticity involved in cerebellar learning; but also that the activity of SK2 channels in particular is required for its expression.

Another important implication of the experiments in Chapter 3 for cerebellar learning is the time scale on which changes in Purkinje cell excitability persist following learning. Most experiments, including those performed in Chapter 2, are looking at stable, but relatively transient expression of intrinsic plasticity lasting anywhere from several minutes to up to an hour. The experiments in Chapter 3, however, show that these changes can persist up to 48 hours following the last experience.

4.3 FUTURE DIRECTIONS

The results presented above, particularly when placed in the context of where the the research into intrinsic plasticity and learning currently stands, raise a number of questions that could be addressed by subsequent experiments.

First of all, as it seems that intrinsic plasticity, as measured by changes in firing rate and AHP, seems to converge on SK2 channel activity in the cerebellum, calcium imaging experiments could be performed to determine whether different forms of synaptic input that lead to varying levels of Ca^{2+} influx into Purkinje cells could be associated greater or lesser SK channel trafficking and therefore expression of intrinsic plasticity. Additionally hippocampus and cortex-dependent forms of learning could be assessed in SK2 global knockout mice to determine if there is a similar deficit in learning as seen when Purkinje cell-specific SK2 knockouts undergo a motor-learning assay. It is important to keep in mind, however, that intrinsic plasticity may not be limited to the changes in excitability observed in these experiments; and that other IP measures may be depended on different ion channels and signaling pathways. While Purkinje cells are excellent for studying

changes in firing rate, due to their high natural activity, other neurons may prove better for studying changes such as firing threshold, resting membrane potential, and sag current.

To further determine how coordination of synaptic and intrinsic plasticity give rise to learning, it would be helpful to block induction of one while studying the other and vice-versa in order to determine if there is an effect on behavior. While the shared induction pathways detailed above might make approach particularly difficult, results such as the different effects of metabotropic facilitation on SD versus synaptic induction suggest that there is a way to tease apart the two mechanisms.

Finally, a behavioral effect of the facilitation effect of metabotropic activity on intrinsic plasticity in particular should be confirmed in Purkinje cells. Although previous research has shown a requirement for mGluR1 activity in cerebellar learning (Aiba et al., 1994; Conquet et al., 1994), these results primarily focused on the role of mGluR1 in LTD (Shigemoto et al., 1994). And while Rinaldo and Hansel (2013) showed that mAChR affects LTP expression in the cerebellum, a corresponding behavioral effect has not yet been identified. Therefore, it is important to confirm both that the effects of metabotropic activity on IP expression seen *in vitro* really do convey meaningful information about the pathway that leads to its induction; and also the role of cholinergic signaling in particular in cerebellar learning.

REFERENCES

A Aiba, M Kano, C Chen, M E Stanton, G D Fox, K Herrup, T A Zwingman, and S Tonegawa. Deficient cerebellar long-term depression and impaired motor learning in mGluR1 mutant mice. *Cell*, 79(2):377–388, October 1994. ISSN 0092-8674. doi: 10.1016/0092-8674(94)90205-4.

D Alkon, I Lederhendler, and J Shoukimas. Primary changes of membrane currents during retention of associative learning, 1982.

Richard Apps and Martin Garwicz. Anatomical and physiological foundations of cerebellar information processing. *Nature reviews. Neuroscience*, 6(4):297–311, April 2005. ISSN 1471-003X. doi: 10.1038/nrn1646.

N H Barmack, R W Baughman, and F P Eckenstein. Cholinergic innervation of the cerebellum of rat, rabbit, cat, and monkey as revealed by choline acetyltransferase activity and immunohistochemistry. *The Journal of comparative neurology*, 317(3):233–249, March 1992. ISSN 0021-9967. doi: 10.1002/cne.903170303.

Amor Belmeguenai, Eric Hosy, Fredrik Bengtsson, Christine M Pedroarena, Claire Piochon, Eva Teuling, Qionger He, Gen Ohtsuki, Marcel T G De Jeu, Ype Elgersma, Chris I De Zeeuw, Henrik Jörntell, and Christian Hansel. Intrinsic plasticity complements long-term potentiation in parallel fiber input gain control in cerebellar Purkinje cells. *Journal of Neuroscience*, 30(41): 13630–13643, October 2010. doi: 10.1523/JNEUROSCI.3226-10.2010.

G Q Bi and M M Poo. Synaptic modifications in cultured hippocampal neurons: dependence on spike timing, synaptic strength, and postsynaptic cell type. *The Journal of neuroscience: the official journal of the Society for Neuroscience*, 18(24):10464–10472, December 1998. ISSN 0270-6474. doi: 10.1038/25665.

R L Brunner and J Altman. Locomotor deficits in adult rats with moderate to massive retardation of cerebellar development during infancy. *Behavioral biology*, 9(2):169–188, August 1973. ISSN 0091-6773. doi: 10.1016/s0091-6773(73)80154-3.

Katherine A Buchanan, Milos M Petrovic, Sophie E L Chamberlain, Neil V Marrion, and Jack R Mellor. Facilitation of Long-Term Potentiation by Muscarinic M1 Receptors Is Mediated by Inhibition of SK Channels. *Neuron*, 68(5):948–963, December 2010. ISSN 0896-6273, 1097-4199. doi: 10.1016/j.neuron.2010.11.018.

Yao Chen, Adam J Granger, Trinh Tran, Jessica L Saulnier, Alfredo Kirkwood, and Bernardo L Sabatini. Endogenous Gαq-Coupled Neuromodulator Receptors Activate Protein Kinase A. *Neuron*, 96(5):1070–1083.e5, December 2017. ISSN 0896-6273. doi: 10.1016/j.neuron.2017.10.023.

Lorenzo A Cingolani, Marco Gymnopoulos, Anna Boccaccio, Martin Stocker, and Paola Pedarzani. Developmental Regulation of Small-Conductance Ca2+-Activated K+ Channel Expression and Function in Rat Purkinje Neurons. *Journal of Neuroscience*, 22(11):4456–4467, 2002. doi: 10.1523/jneurosci.22-11-04456.2002.

F Conquet, Z I Bashir, C H Davies, H Daniel, F Ferraguti, F Bordi, K Franz-Bacon, A Reggiani, V Matarese, and F Condé. Motor deficit and impairment of synaptic plasticity in mice lacking mGluR1. *Nature*, 372(6503):237–243, November 1994. ISSN 0028-0836. doi: 10.1038/372237a0.

Ana P Crestani, Jamie N Krueger, Eden V Barragan, Yuki Nakazawa, Sonya E Nemes, Jorge A Quillfeldt, John A Gray, and Brian J Wiltgen. Metaplasticity contributes to memory formation in the hippocampus. *Neuropsychopharmacology: official publication of the American College of Neuropsychopharmacology*, 44(2):408–414, May 2019. ISSN 0893-133X. doi: 10.1038/s41386-018-0096-7.

Dominique Debanne and Michaël Russier. The contribution of ion channels in input-output plasticity. *Neurobiology of learning and memory*, 166(September):107095–107095, September 2019. ISSN 1074-7427. doi: 10.1016/j.nlm.2019.107095.

Steven N Duffy and Peter V Nguyen. Postsynaptic application of a peptide inhibitor of cAMP-dependent protein kinase blocks expression of long-lasting synaptic potentiation in hippocampal neurons. *The Journal of neuroscience: the official journal of the Society for Neuroscience*, 23(4):1142–1150, February 2003. ISSN 0270-6474, 1529-2401. doi: 10.1523/JNEUROSCI.23-04-01142.2003.

Veronica C Galvin, Sheng Tao Yang, Constantinos D Paspalas, Yang Yang, Lu E Jin, Dibyadeep Datta, Yury M Morozov, Taber C Lightbourne, Adam S Lowet, Pasko Rakic, Amy F T Arnsten, and Min Wang. Muscarinic M1 Receptors Modulate Working Memory Performance and Activity via KCNQ Potassium Channels in the Primate Prefrontal Cortex. *Neuron*, 106(4):649–661.e4, May 2020. ISSN 0896-6273, 1097-4199. doi: 10.1016/j.neuron.2020.02.030.

Zhenyu Gao, Boeke J van Beugen, and Chris I De Zeeuw. Distributed synergistic plasticity and cerebellar learning. *Nature reviews. Neuroscience*, 13(9):619–635, September 2012. ISSN 1471-003X, 1471-0048. doi: 10.1038/nrn3312.

Giorgio Grasselli, Qionger He, Vivian Wan, John P Adelman, Gen Ohtsuki, and Christian Hansel. Activity-Dependent Plasticity of Spike Pauses in Cerebellar Purkinje Cells. *Cell reports*, 14 (11):2546–2553, March 2016. doi: 10.1016/j.celrep.2016.02.054.

Giorgio Grasselli, Henk-Jan Boele, Heather K Titley, Nora Bradford, Lisa van Beers, Lindsey Jay, Gerco C Beekhof, Silas E Busch, Chris I de Zeeuw, Martijn Schonewille, and Christian Hansel. SK2 channels in cerebellar Purkinje cells contribute to excitability modulation in motor-learning-specific memory traces. *PLoS biology*, 18(1):e3000596, January 2020. ISSN 1544-9173, 1545-7885. doi: 10.1371/journal.pbio.3000596.

M Ito. Cerebellar learning in the vestibulo-ocular reflex. *Trends in cognitive sciences*, 2(9):313–321, September 1998. ISSN 1364-6613. doi: 10.1016/s1364-6613(98)01222-4.

Dick Jaarsma, Tom J H Ruigrok, Romeo Caffé, Constantino Cozzari, Allan I Levey, Enrico Mugnaini, and Jan Voogd. Chapter 5 Cholinergic innervation and receptors in the cerebellum. In C I De Zeeuw, P Strata, and J Voogd, editors, *Progress in Brain Research*, volume 114 of

Progress in brain research, pages 67–96. Elsevier, January 1997. ISBN 9780444823137. doi: 10.1016/S0079-6123(08)63359-2.

Henrik Jörntell and Christian Hansel. Synaptic Memories Upside Down: Bidirectional Plasticity at Cerebellar Parallel Fiber-Purkinje Cell Synapses, October 2006.

Sheena A Josselyn and Susumu Tonegawa. Memory engrams: Recalling the past and imagining the future. *Science*, 367(6473), January 2020. ISSN 0036-8075, 1095-9203. doi: 10.1126/science.aaw4325.

Varda Lev-Ram, Scott T Wong, Daniel R Storm, and Roger Y Tsien. A new form of cerebellar long-term potentiation is postsynaptic and depends on nitric oxide but not cAMP. *Proceedings of the National Academy of Sciences of the United States of America*, 99(12):8389–8393, June 2002. ISSN 0027-8424. doi: 10.1073/pnas.122206399.

Carmen Lin, John Disterhoft, and Craig Weiss. Whisker-signaled Eyeblink Classical Conditioning in Head-fixed Mice. *Journal of visualized experiments: JoVE*, (109):e53310, March 2016. ISSN 1940-087X. doi: 10.3791/53310.

Rafael Luján, Carolina Aguado, Francisco Ciruela, Xavier Morató Arus, Alejandro Martín-Belmonte, Rocío Alfaro-Ruiz, Jesús Martínez-Gómez, Luis de la Ossa, Masahiko Watanabe, John P Adelman, Ryuichi Shigemoto, and Yugo Fukazawa. SK2 Channels Associate With mGlu1α Receptors and CaV2.1 Channels in Purkinje Cells. *Frontiers in cellular neuroscience*, 12:311–311, September 2018. doi: 10.3389/fncel.2018.00311.

James Maylie and John P Adelman. Cholinergic Signaling through Synaptic SK Channels: It's a Protein Kinase but Which One? *Neuron*, 68(5):809–811, 2010. ISSN 0896-6273, 1097-4199. doi: 10.1016/j.neuron.2010.11.037.

D A McCormick and R F Thompson. Neuronal responses of the rabbit cerebellum during acquisition and performance of a classically conditioned nictitating membrane-eyelid response. *The Journal of neuroscience: the official journal of the Society for Neuroscience*, 4(11):2811–2822, November 1984. ISSN 0270-6474.

J R Moyer, Jr, L T Thompson, and J F Disterhoft. Trace eyeblink conditioning increases CA1 excitability in a transient and learning-specific manner. *The Journal of neuroscience: the official journal of the Society for Neuroscience*, 16(17):5536–5546, September 1996. ISSN 0270-6474. doi: 10.1523/JNEUROSCI.16-17-05536.1996.

Heeyoun Park, Taegon Kim, Jinhyun Kim, Yukio Yamamoto, Heeyoun Park, Taegon Kim, Jinhyun Kim, Yukio Yamamoto, and Keiko Tanaka-yamamoto. Inputs from Sequentially Developed Parallel Fibers Are Required for Cerebellar Organization Article Inputs from Sequentially Developed Parallel Fibers Are Required for Cerebellar Organization. *CellReports*, 28(11):2939–2954.e5, September 2019. doi: 10.1016/j.celrep.2019.08.010.

Yajun Ren, Lyndon F Barnwell, Jon C Alexander, Farah D Lubin, John P Adelman, Paul J Pfaffinger, Laura A Schrader, and Anne E Anderson. Regulation of surface localization of the small

conductance Ca 2+-activated potassium channel, Sk2, through direct phosphorylation by cAMP-dependent protein kinase. *The Journal of biological chemistry*, 281(17):11769–11779, April 2006. ISSN 0021-9258. doi: 10.1074/jbc.M513125200.

Lorenzo Rinaldo and Christian Hansel. Muscarinic acetylcholine receptor activation blocks long-term potentiation at cerebellar parallel fiber-Purkinje cell synapses via cannabinoid signaling. *Proceedings of the National Academy of Sciences of the United States of America*, 110(27): 11181–11186, July 2013. ISSN 0027-8424, 1091-6490. doi: 10.1073/pnas.1221803110.

B G Schreurs, P A Gusev, D Tomsic, D L Alkon, and T Shi. Intracellular correlates of acquisition and long-term memory of classical conditioning in Purkinje cell dendrites in slices of rabbit cerebellar lobule HVI. *The Journal of neuroscience: the official journal of the Society for Neuroscience*, 18(14):5498–5507, 1998. ISSN 0270-6474. doi: 10.1523/JNEUROSCI.18-14-05498.1998.

Bernard G Schreurs. Changes in cerebellar intrinsic neuronal excitability and synaptic plasticity result from eyeblink conditioning. *Neurobiology of learning and memory*, 166(September): 107094–107094, September 2019. ISSN 1074-7427. doi: 10.1016/j.nlm.2019.107094.

R Shigemoto, T Abe, S Nomura, S Nakanishi, and T Hirano. Antibodies inactivating mGluR1 metabotropic glutamate receptor block long-term depression in cultured Purkinje cells. *Neuron*, 12(6):1245–1255, June 1994. ISSN 0896-6273. doi: 10.1016/0896-6273(94)90441-3.

Hyun Geun Shim, Dong Cheol Jang, Jaegeon Lee, Geehoon Chung, Sukchan Lee, Yong Gyu Kim, Da Eun Jeon, and Sang Jeong Kim. Long-term depression of intrinsic excitability accompanied by synaptic depression in cerebellar purkinje cells. *Journal of Neuroscience*, 37(23):5659–5669, June 2017. doi: 10.1523/JNEUROSCI.3464-16.2017.

Aparna Suvrathan, Hannah L Payne, and Jennifer L Raymond. Timing Rules for Synaptic Plasticity Matched to Behavioral Function. *Neuron*, 97(1):248–250, January 2018. ISSN 0896-6273, 1097-4199;0896-6273. doi: 10.1016/j.neuron.2017.12.019.

Alexander Thiele. Muscarinic signaling in the brain. *Annual review of neuroscience*, 36:271–294, July 2013. ISSN 0147-006X, 1545-4126. doi: 10.1146/annurev-neuro-062012-170433.

L T Thompson, J R Moyer, Jr, and J F Disterhoft. Transient changes in excitability of rabbit CA3 neurons with a time course appropriate to support memory consolidation. *Journal of neurophysiology*, 76(3):1836–1849, September 1996. ISSN 0022-3077. doi: 10.1152/jn.1996.76.3.1836.

Heather K Titley, Nicolas Brunel, and Christian Hansel. Toward a Neurocentric View of Learning, July 2017.

Ruben S Van Der Giessen, Sebastiaan K Koekkoek, Stijn van Dorp, Jornt R De Gruijl, Alexander Cupido, Sara Khosrovani, Bjorn Dortland, Kerstin Wellershaus, Joachim Degen, Jim Deuchars, Elke C Fuchs, Hannah Monyer, Klaus Willecke, Marcel T G De Jeu, and Chris I De Zeeuw. Role of olivary electrical coupling in cerebellar motor learning. *Neuron*, 58(4):599–612, May 2008. ISSN 0896-6273, 1097-4199. doi: 10.1016/j.neuron.2008.03.016.

Mark J Wagner and Liqun Luo. Neocortex–Cerebellum Circuits for Cognitive Processing. *Trends in neurosciences*, November 2019. ISSN 0166-2236. doi: 10.1016/j.tins.2019.11.002.

Adelaide P Yiu, Valentina Mercaldo, Chen Yan, Blake Richards, Asim J Rashid, Hwa Lin Liz Hsiang, Jessica Pressey, Vivek Mahadevan, Matthew M Tran, Steven A Kushner, Melanie A Woodin, Paul W Frankland, and Sheena A Josselyn. Neurons Are Recruited to a Memory Trace Based on Relative Neuronal Excitability Immediately before Training. *Neuron*, 83(3):722–735, August 2014. ISSN 0896-6273. doi: 10.1016/j.neuron.2014.07.017.